PUBLICATIONS OF THE ASTRONOMICAL SOCIETY OF THE PACIFIC, **124**:140–157, 2012 February

Spectrophotometric Libraries, Revised Photonic Passbands, and Zero Points for *UBVRI*, *Hipparcos*, and Tycho Photometry

MICHAEL BESSELL AND SIMON MURPHY

Research School of Astronomy and Astrophysics, Mount Stromlo Observatory, The Australian National University, ACT 2611, Australia; bessell@mso.anu.edu.au

Received 2011 September 16; accepted 2011 December 8; published 2012 February 8

ABSTRACT. We have calculated improved photonic passbands for the $UBVRI$, *Hipparcos* H_p, and Tycho B_T and V_T standard systems using the extensive spectrophotometric libraries of NGSL and MILES. Using the H_p passband, we adjusted the absolute flux levels of stars in the spectrophotometric libraries so that their synthetic H_p magnitudes matched the precise *Hipparcos* Catalogue value. Synthetic photometry based on the renormalized fluxes was compared with the standard $UBVRI$, B_T and V_T magnitudes, and revised synthetic zero points were determined. The *Hipparcos* and Tycho photometry system zero points were also compared with the V-magnitude zero points of the SAAO $UBVRI$ system, the homogenized UBV system, and the Walraven VB system. The confusion in the literature concerning broadband magnitudes, fluxes, passbands, and the choice of appropriate mean wavelengths is detailed and discussed in the Appendix.

Online material: color figures, extended tables

1. INTRODUCTION

The *Hipparcos* Catalogue (Perryman et al. 1997) is a high-precision photometric (plus parallax and proper motion) catalog of more than 100,000 stars measured with the H_p band; the Tycho2 Catalogue (Hog et al. 2000) contains 2.5 million stars measured (mostly) with lower precision in the B_T and V_T bands. The remarkable collection of data was obtained during the 4 yr (1989–1993) mission of the *Hipparcos* satellite. The *Hipparcos* and Tycho photometric systems and their measured median precisions were discussed by van Leeuwen et al. (1997b), and the passbands were given in van Leeuwen et al. (1997a). However, the detectors suffered degradation throughout the mission as a result of being launched into an incorrect orbit, and this degradation invalidated the measured prelaunch passbands. Bessell (2000) devised self-consistent *Hipparcos* and Tycho passbands by comparing regressions of $V - H_p$, $V - B_T$, and $V - V_T$ versus $V - I$ for a sample of precise E-region $UBVRI$ standard stars with synthetic photometry computed from the $R \sim 100$ Vilnius-averaged spectra (Straizys & Sviderskiene 1972). This indicated the necessity of a significant redward shift of the blue edge of the published H_p band, but only small changes for the Tycho bands. However, the passbands may not have been definitive because of the small number of averaged Vilnius spectra used and their low resolution.

In the last few years, two libraries of accurate higher-resolution ($R \sim 1000$–2000) spectrophotometric data have become available—the Next Generation Spectral Library[1] (NGSL; Heap & Lindler 2007) and the Medium Resolution INT Library of Empirical Spectra[2] (MILES; Sanchez-Blazquez et al. 2006. Many of the stars in these spectral libraries also have *Hipparcos* and Tycho magnitudes—providing the opportunity to reexamine the passbands of the *Hipparcos* and Tycho systems. Furthermore, the high precision of the *Hipparcos* magnitudes (Perryman et al. 1997) enables them to be used to adjust the flux levels of the data in the NGSL libraries and to make the stars extremely valuable for whole-sky spectrophotometric calibration of imaging surveys such as SkyMapper (Keller et al. 2007).

Being space-based, a unique property of the *Hipparcos* photometric systems is the absence of any seasonal or hemisphere-related effects seen in some ground-based photometric systems due to variations in temperature, atmospheric extinction, and instrumental orientation. The *Hipparcos* photometry database can therefore be compared with databases of ground-based photometric systems to examine their magnitude zero points and to look for any systematic offsets in the photometry, as discussed by van Leeuwen et al. (1997a) and Pel & Lub (2007).

In this article, we will outline the derivation of improved $UBVRI$, *Hipparcos*, and Tycho passbands by using synthetic photometry from spectrophotometric atlases and comparing it

[1] See http://archive.stsci.edu/prepds/stisngsl/index.html.
[2] See http://www.iac.es/proyecto/miles/.

with broadband photometry. We will also adjust the absolute levels of the spectrophotometric fluxes by comparing the synthesized H_p magnitudes with the *Hipparcos* Catalogue magnitudes. In addition, we will use the mean differences between the synthetic and the observed photometry to determine zero-point corrections for the $UBVRI$ B_T and V_T bands. We will also intercompare the zero points of the SAAO $UBVRI$, the homogenized UBV, and the Walraven VB systems. Finally, in the Appendix we discuss confusion and inexactness concerning the derivation of mean fluxes, response functions, and the plethora of expressions for mean wavelengths and frequencies associated with broadband photometry.

2. SYNTHETIC PHOTOMETRY

The synthetic photometry in this article was computed using two photometry packages.[3] For each passband x, we evaluated the quantity

$$\mathrm{mag}_x = \mathrm{AB} - \mathrm{ZP}_x, \tag{1}$$

where

$$\begin{aligned}\mathrm{AB} &= -2.5\log\frac{\int f_\nu(\nu)S_x(\nu)d\nu/\nu}{\int S_x(\nu)d\nu/\nu} - 48.60\\ &= -2.5\log\frac{\int f_\lambda(\lambda)S_x(\lambda)\lambda d\lambda}{\int S_x(\lambda)cd\lambda/\lambda} - 48.60,\end{aligned} \tag{2}$$

$f_\nu(\nu)$ is the observed absolute flux in erg cm^{-2} s^{-1} Hz^{-1}, $f_\lambda(\lambda)$ is the observed absolute flux in erg cm^{-2} s^{-1} Å^{-1}, $S_x(\lambda)$ are the photonic passbands (response functions), λ is the wavelength in angstroms, and ZP_x are the zero-point magnitudes for each band (see §§ 5.4 and 7 and the Appendix). For SI units the constants in the preceding equations would be different, because erg cm^{-2} s^{-1} is equivalent to 10^{-3} W m^{-2}.

For accurate synthetic photometry it is important that the passbands provided to the integration routines are well sampled and smooth. Because passbands are usually published at coarse wavelength intervals (25–100 Å), it is necessary to interpolate these passband tables to a finer spacing of a few angstroms using a univariate spline or a parabolic interpolation routine. The physical passbands themselves are smooth, and the recommended interpolation recovers this. Our two packages produced identical results after this step.

3. COMPLICATIONS AND CAVEATS TO THE REALIZATION OF STANDARD SYSTEMS

There is a fundamental concern associated with the theoretical realization of the older evolved standard photometric systems in order to produce synthetic photometry from theoretical and observational fluxes. The technique used is to reverse-engineer the standard system's passband sensitivity functions by comparing synthetic photometry with observations (e.g., Straižys 1996; $UBVRIJHKL$: Bessell 1990a; Bessell & Brett 1988). That is, commencing with a passband based on an author's prescription of detector and filter bandpass, synthetic magnitudes are computed from absolute or relative-absolute spectrophotometric fluxes for stars with known standard colors. By slightly modifying the initial passband (shifting the central wavelength or altering the blue or red cutoff) and recomputing the synthetic colors, it is usually possible to devise a bandpass that generates magnitudes that differ from the standard magnitudes *within the errors* by only a constant that is independent of the color of the star. It is usually taken for granted that such a unique passband exists and that given a large enough set of precise spectrophotometric data and sufficient passband adjustment trials, it can be recovered. However, there are several reasons why this may not be the case, at least not across the complete temperature range.

Although the original system may have been based on a real set of filters and detector, the original set of standard stars would almost certainly have been obtained with lower precision than is now possible and for stars of a restricted temperature and luminosity range. The filters may also have been replaced during the establishment of the system, and the later data may have been linearly transformed onto mean relations shown by the previous data. In addition, the contemporary lists of very high precision secondary standards that essentially define the standard systems have all been measured using more sensitive equipment, with different wavelength responses. Again, rather than preserve the natural scale of the contemporary equipment, the measurements have been "transformed" to some mean representation of the original system by applying one or more linear transformations or even nonlinear transformations (e.g., Menzies 1993). To incorporate bluer or redder stars than those in the original standard lists (e.g., Kilkenny et al. 1998), extrapolations have also been made, and these may have been unavoidably skewed by the imprecision of the original data and the small number of stars with extreme colors in the original lists. As a result, the contemporary standard system, *although well defined observationally* by lists of stars with precise colors and magnitudes, *may not represent any real system* and is therefore impossible to realize with a unique passband that can reproduce the standard magnitudes and colors through a linear transformation with a slope of 1.0.

In fact, perhaps we should not be trying to find a unique passband with a central wavelength and shape that can reproduce the colors of a standard system, but we should rather be trying to match the passbands and the linear (but nonunity slope) or nonlinear transformations used by the contemporary standard system authors to transform their natural photometry onto the standard system. The revised realization of the Geneva photometric system by Nicolet (1996) uses this philosophy, as does Bessell (2011) in the realization of the $uvby$ system.

[3] One was written in 1980 by Andrew Pickles, and the other is pysynphot (see http://stsdas.stsci.edu/pysynphot). Version 0.9 is distributed as part of stsci-python 2.12 (2011 August).

However, in this article we have set out in the traditional way, as outlined previously, to adjust the passbands to achieve agreement between the synthetic photometry and the standard system photometry within the errors of the standard system. It may seem desirable to do these passband adjustments in a less ad hoc way, but given the uncertainties underlying existing standard system photometry, a more accurate method is unnecessary, at present.

4. THE NGSL AND MILES SPECTRA

Because of how spectroscopic observations are normally made, spectrophotometric fluxes are calibrated mainly to determine the accurate relative-absolute fluxes (the flux variation with wavelength), but not the absolute flux (the apparent magnitude). Depending on the slit width and the seeing or other instrumental effects, the resultant absolute flux levels may be measured only to a precision of 0.1–0.2 mag. To assign an accurate absolute flux level, one is normally required to compute a synthetic magnitude from the spectrophotometric fluxes and to equate this to a standard magnitude for the object, often an existing magnitude, such as B or V. Currently, the most precise magnitudes available for the largest number of stars are the *Hipparcos* H_p magnitudes. There are 72,300 stars in the *Hipparcos* Catalogue, with median H_p magnitudes given to better than 0.002 mag. We have therefore synthesized the H_p magnitudes for all the stars in the spectrophotometric libraries and adjusted the absolute flux scale of each star (that is in the *Hipparcos* Catalogue) to match the catalog H_p value, thus producing spectrophotometric data with an uncertainty in the overall absolute flux level of a few millimagnitudes. In Figure 1 we show histograms of the differences for the NGSL stars between the observed and synthetic V magnitudes before and after renormalization to the H_p magnitudes. We could not show this comparison for the MILES spectra, as they published only relative-absolute fluxes (normalized to 1 at 4600 Å), but after renormalization to the H_p magnitudes, the ΔV distributions for both NGSL and MILES spectral libraries are approximately Gaussian, with a similar rms of 0.017 mag.

The wavelength range of the NGSL spectra encompasses the wavelength range of the *Hipparcos* and Tycho passbands, but because the MILES spectra do not cover the complete extent of the red tails of the H_p and the R band, or any of the I band, we have extrapolated the MILES spectra from 7000 Å to 9900 Å using model atmosphere fits to the 3500 Å–7000 Å region by Kerzendorf (2011, private communication). The grids used were from ATLAS (Munari et al. 2005) for $T_{\rm eff} > 8000$ K and MARCS (Gustafsson et al. 2008) for $8000\ {\rm K} > T_{\rm eff} > 2500$ K. The MILES spectra were also extrapolated from 3540 Å to 3000 Å to cover the U band. These extrapolations may result in a slight uncertainty in the synthetic photometry in some passbands from the MILES spectra; however, we think that it is small, as shown by the insignificant differences

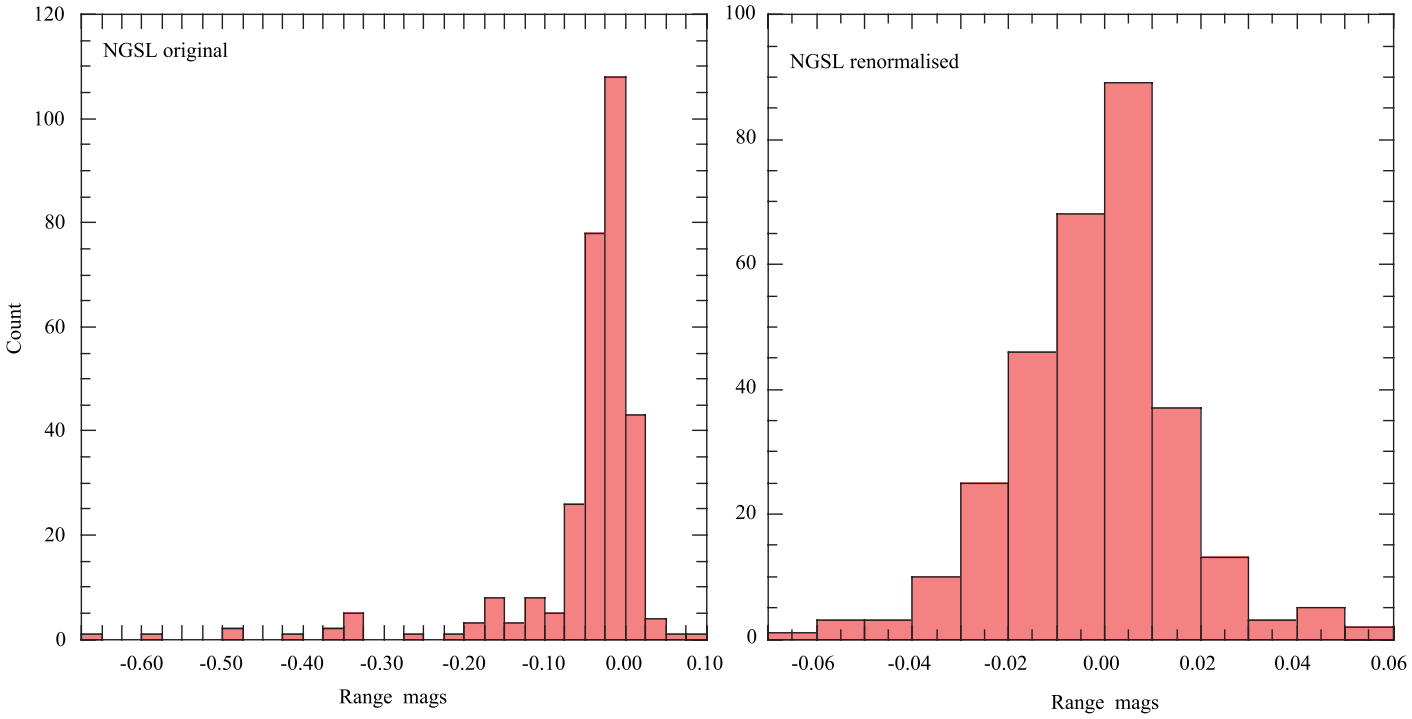

FIG. 1.—Histogram of difference between observed and synthetic V magnitudes for original NGSL spectra (*left*) and renormalized spectra (*right*). The renormalized MILES spectra show a very similar distribution and rms. See the electronic edition of the *PASP* for a color version of this figure.

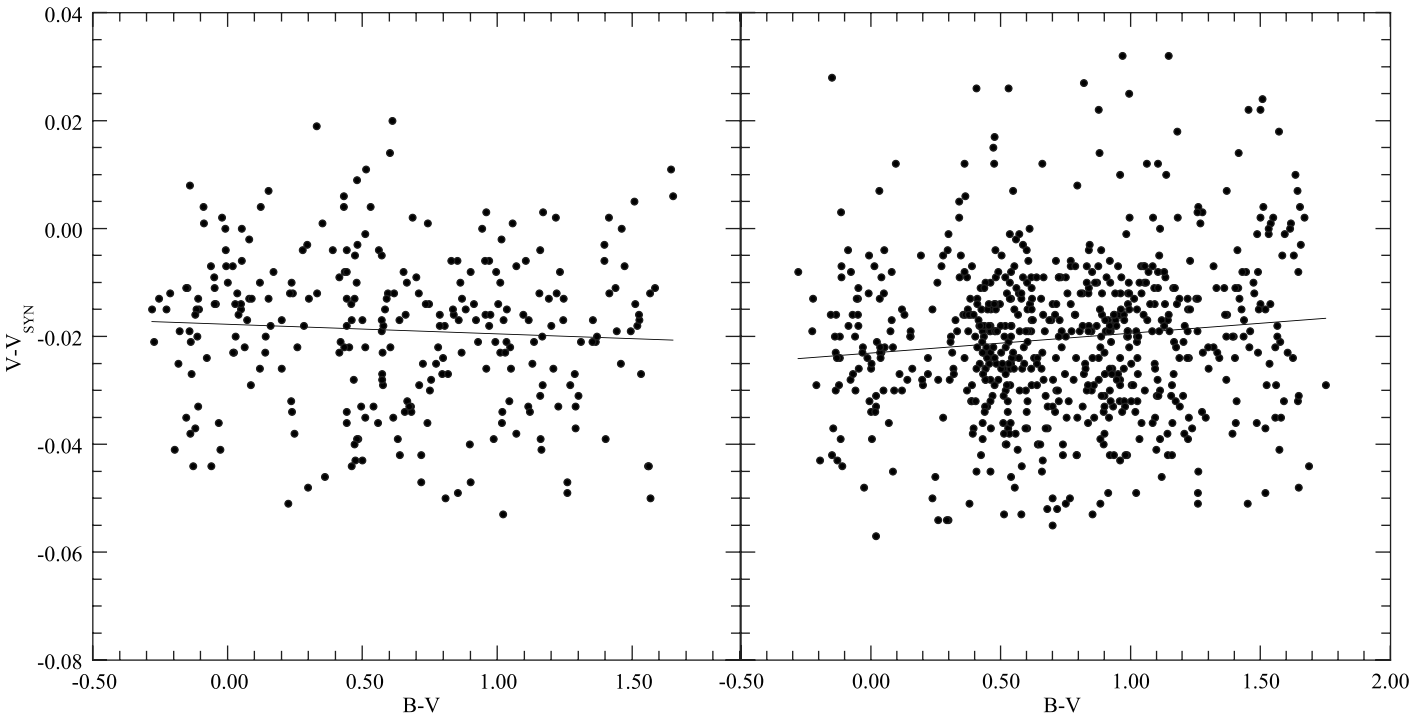

FIG. 2.—Difference between observed and synthetic V magnitudes for NGSL (*left*) and MILES (*right*) samples. The solid lines show linear fits to the data.

between the relations using the NGSL and MILES spectra, probably except for the M stars.

The 373 adjusted NGSL spectrophotometric fluxes, covering the wavelength range 1800 Å to 10,100 Å and with a precise absolute flux level, are ideally suited to calibrate whole-sky surveys, such as SkyMapper (Keller et al. 2007) and Pan-STARRS (Kaiser et al. 2010). These revised absolute fluxes are available from the authors, together with the absolute fluxes for the 836 MILES spectra that have *Hipparcos* photometry.

5. THE *UBVRI* PASSBANDS

The Johnson-Cousins $UBVRI$ system passbands have been well discussed (e.g., Azusienis & Straizys 2009; Buser & Kurucz 1978; Bessell 1990a), most recently, by Maiz Appellaniz (2006), who reconsidered the UBV passbands. Although accepting the Bessell (1990a) BV passbands, Maiz Appelaniz (2006) suggested an unusual and unphysical U passband as providing a better fit to standard U photometry. However, these previous analyses did not have available the large number of revised spectra in the NGSL and the MILES catalogs. It is very worthwhile, therefore, to reexamine the $UBVRI$ passbands using synthetic $UBVRI$ photometry derived from these extensive data sets. Standard system UBV data for most of the MILES and NGSL stars are available in the homogenized UBV catalog.[4] VI data are available for many stars in the *Hipparcos* Catalogue, while various data sets of Cousins, Menzies, Landolt, Bessell, Kilkenny, and Koen also provided much supplementary VRI data (Cousins 1974, 1976, 1984; Cousins & Menzies 1993; Landolt 1983, 2009; Bessell 1990b; Kilkenny et al. 1998; Koen et al. 2002, 2010).

5.1. The *B* and *V* Passbands

After comparing the observed and synthetic photometry, very small slopes were evident in the ΔB and ΔV regressions against $B-V$ using the Bessell (1990a) passbands with the NGSL and MILES samples. These slopes were removed by making a small redward shift to the red side of the $V90$ band and a very small overall redward shift in the $B90$ band. The regressions for the MILES sample were similar but not identical. In Figures 2 and 3 for the NGSL spectra we show the differences between the observed and synthetic V and $B-V$, respectively, for our adopted passbands. There are no significant color terms evident, but the synthetic $V$and $B-V$ magnitude scales have small apparent offsets associated with the initial adopted zero points (hereinafter ZPs) of the synthetic photometry. These will be addressed further in § 7.

5.2. The *U* Bandpass Revisited

Standard U photometry has a bad reputation due to the much larger systematic differences in $U-B$ between observers than is evident for V and $B-V$. These systematic differences arise because in stars, U measures the flux across the region of the

[4] Vizier Online Data Catalog, II/168 (J. C. Mermilliod, 2006).

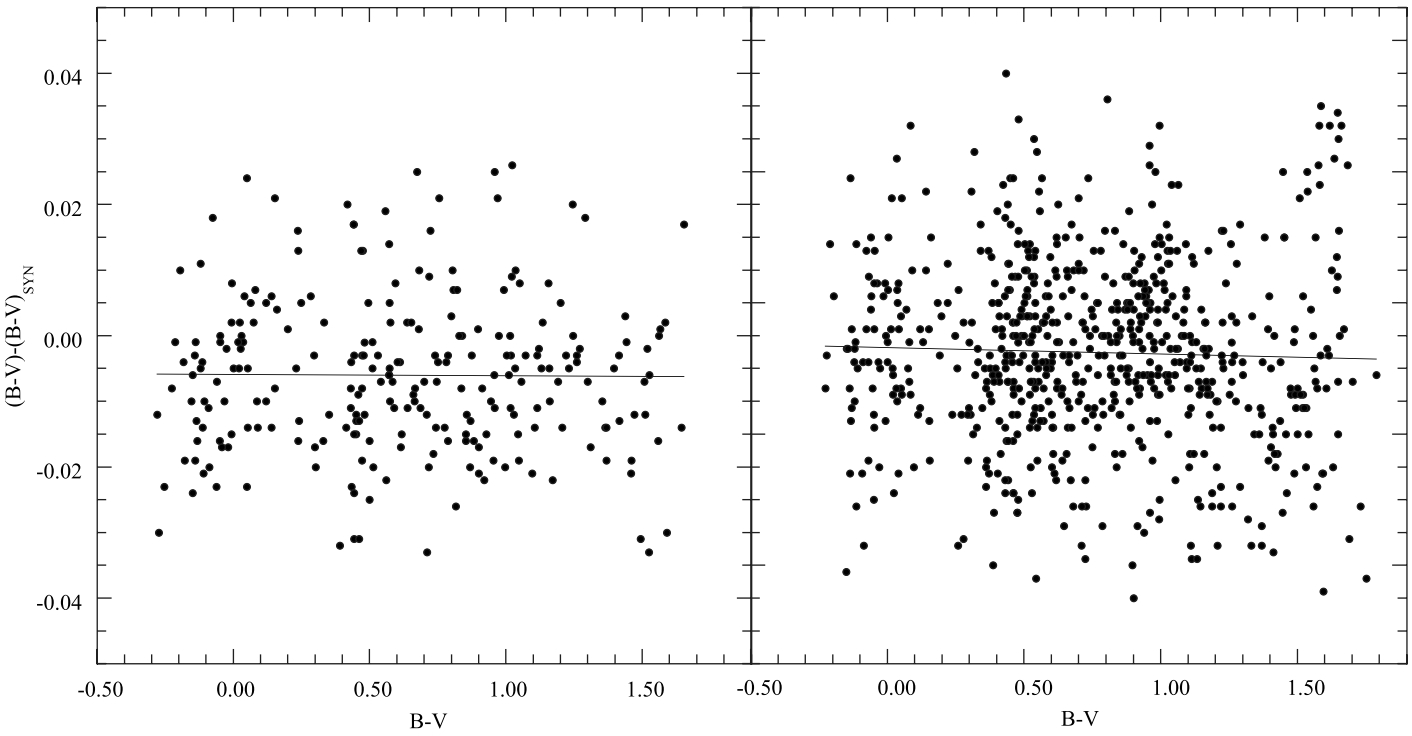

FIG. 3.—Difference between observed and synthetic $B-V$ for NGSL (*left*) and MILES (*right*) samples. The solid lines show linear fits to the data.

Balmer jump, and its response is therefore much more sensitive to the exact placement of the band compared with the placement of B and V. Many observers take insufficient care to match the position and width of the standard Cousins or Johnson U passband, and attempts to standardize the resulting $U-B$ color using a single $B-V$ or $U-B$ color-correction term have introduced systematic errors, especially for reddened stars. Cousins (1984) (reprised in Bessell 1990a) outlined such systematic differences evident in different versions of the $U-B$ system.

Bessell (1986, 1990a) discussed in detail the likely response function of the U band from first principles and proposed the $UX90$ band as representing the original band. Bessell et al. (1998) note that the $U-B$ based on this band should be scaled by 0.96. Although scaling of this order is common in transforming observational systems (e.g., Menzies 1993; Landolt 1983), there is a notable reluctance to use such terms in computing synthetic photometry. In spite of the evidence that most standard systems have evolved with nonlinear or bilinear correction terms (Bessell et al. 1998, Appendix E1), most astronomers believe that a passband can be found that reproduces the standard system without the need for linear and/or nonlinear correction terms. In the spirit of that quixotic endeavor, Buser & Kurucz (1978) and Maiz Appellaniz (2006) proposed U passbands that have almost identical red cutoffs to the $UX90$ band, but different UV cutoffs, thus shifting the effective wavelength of U slightly redward. We have also produced a slightly different U band by moving the UV cutoff of the $UX90$ band slightly redward. This produces an acceptable compromise for the U band that fits the observations reasonably well, although a nonlinear fit would be better.

In Figure 4, we show regressions against $U-B$ of the differences between the U photometry synthesized with the passband from this article and those of Bessell (1990a):$UX90$, Buser &

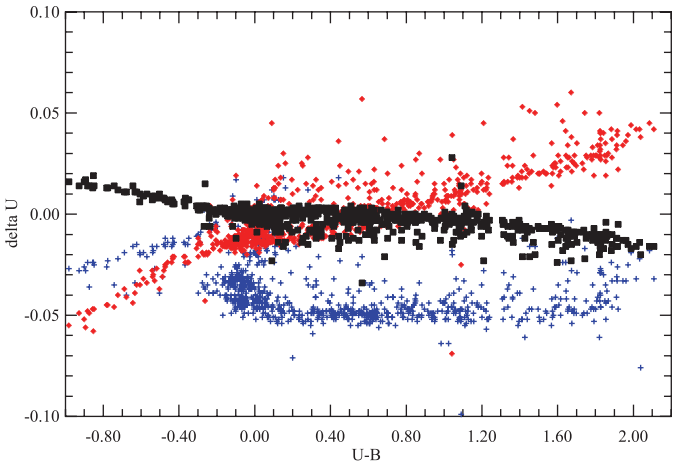

FIG. 4.—Differences in the MILES sample synthetic U magnitudes computed with the U passband in this article and those of Bessell (1990a): $UX90$ (*squares*), Buser & Kurucz (1978): $U3$ (*diamonds*), Maiz Appellaniz (2006) (*crosses*). See the electronic edition of the *PASP* for a color version of this figure.

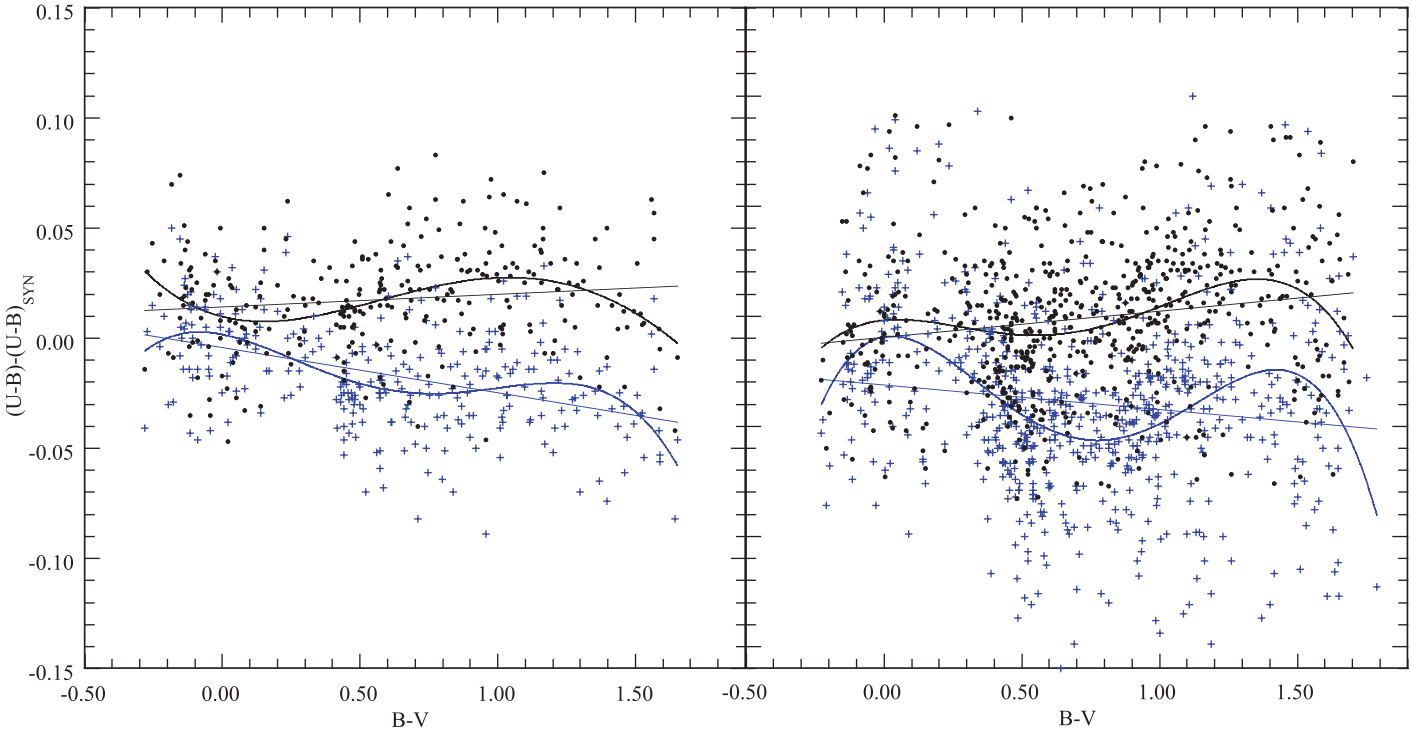

FIG. 5.—Differences between observed $U - B$ and synthetic $U - B$ for the NGSL (*left*) and MILES (*right*) sample of stars computed with the U passband in this article (*dots*) and Maiz Appellaniz (2006) (*crosses*). The solid lines show the linear and fourth-order fits to the differences. See the electronic edition of the *PASP* for a color version of this figure.

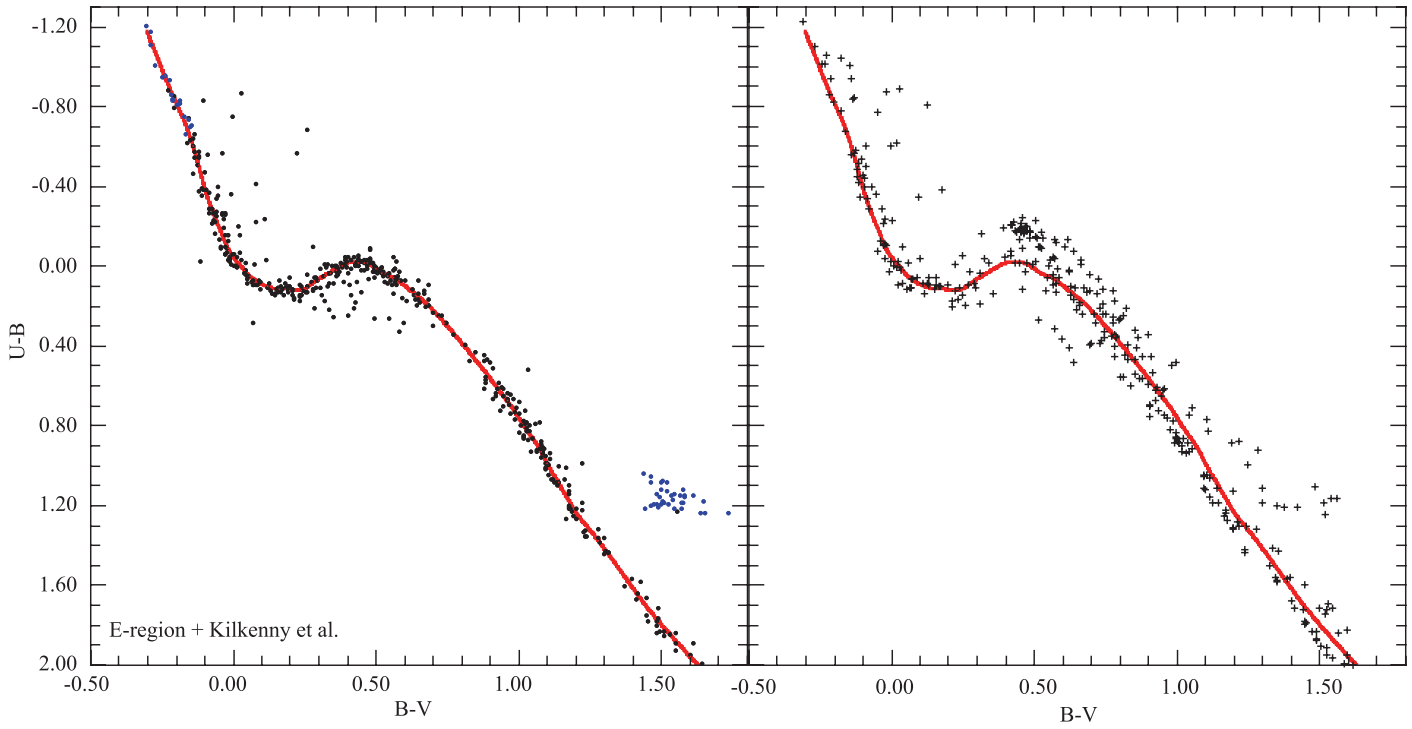

FIG. 6.—*Left*: Standard $U - B$ vs. $B - V$ relation, E-region stars (*black dots*), and additional blue and red dwarfs (*medium-gray dots*). *Right*: Synthetic $U - B$ vs. $B - V$ relation for adopted passbands and the NGSL stars. The thick line is the same in both figures. The metal-deficient stars in the NGSL sample lie above the fiducial line for $B - V$ between 0.3 and 1.0. See the electronic edition of the *PASP* for a color version of this figure.

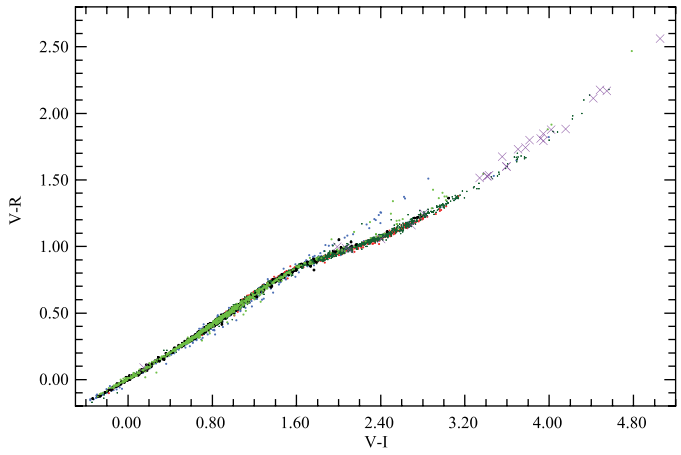

FIG. 7.—Comparison between empirical and synthetic $V-R$ vs. $V-I$ relations. Empirical data: Landolt (2009)—dark-gray dots, Koen et al. (2010)—medium-gray dots, and Bessell (1990b)—plusses. Synthetic data: NGSL—squares, MILES—light-gray dots, and DBS M dwarf spectrophotometry—crosses. See the electronic edition of the *PASP* for a color version of this figure.

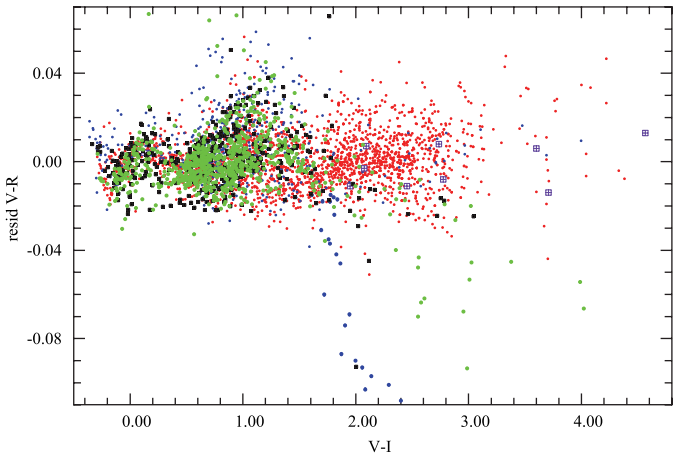

FIG. 8.—Comparison between the residuals of the same ninth-order polynomial fit to the synthetic and catalog $V-R$ vs. $V-I$ relations (see text for details). Synthetic photometry: NGSL—squares, MILES—large light-gray dots, and DBS M dwarfs spectra—crossed boxes. Observed photometry: E-region stars (Menzies et al. 1989; Menzies 1990, private communication)—small gray dots, K and M dwarfs (Koen et al. 2010; Bessell 1990a)—small gray dots, and Landolt (2009) dwarfs—small dark-gray dots, giants—larger large dark-gray dots. See the electronic edition of the *PASP* for a color version of this figure.

Kurucz (1978):$U3$, and Maiz Appellaniz (2006). The main difference between Bessell (1990a) and Buser & Kurucz (1978) is a small difference in slope, whereas the Maiz Appellaniz (2006) passband mainly produces an offset of about 0.05 mag for G, K, and M stars compared with the A and B stars.

In Figure 5, we show the differences between the observed values of $U-B$ and the synthetic $U-B$ computed for the NGSL and MILES sample of stars. Although the scatter is quite high, the Maiz Appellaniz (2006) U passband clearly does less well and results in a systematic deviation from the standard system for the cooler stars (as anticipated in Fig. 4).

The SAAO $UBVRI$ photometry (Cousins 1974, 1976; Kilkenny et al. 1998; Koen et al. 2002, 2010) represents some of the best standard $UBVRI$ photometry, and we use the $U-B$ versus $B-V$ relation from these data (Fig. 6, left panel) as the benchmark for comparison with the synthetic photometry. The Kilkenny et al. (1998) photometry (*dots*) extended the standard system to much bluer and redder dwarf stars than are represented in the E-region stars (*dots*). The line is a fitted mean line through the O-B-A-F-G dwarf main sequence and the K and M giants. In the right panel of Figure 6, the same line is drawn for comparison on the synthetic $U-B$ versus $B-V$ diagram computed for the NGSL sample of stars using our adopted UBV passbands. Considering that there are many metal-deficient F, G, and K stars in the NGSL sample that are not in the empirical sample, the synthetic diagram is in good agreement with the empirical diagram. Note also that most of the reddest stars in the NGSL sample are K and M giants, and there are only a few K and M dwarfs.

TABLE 1
NORMALIZED $UBVRI$ PHOTONIC RESPONSES

Wave	U	Wave	B	Wave	V	Wave	R	Wave	I
3000	0.000	3600	0.000	4700	0.000	5500	0.000	7000	0.000
3050	0.019	3700	0.031	4800	0.033	5600	0.247	7100	0.090
3100	0.068	3800	0.137	4900	0.176	5700	0.780	7200	0.356
3150	0.167	3900	0.584	5000	0.485	5800	0.942	7300	0.658
3200	0.278	4000	0.947	5100	0.811	5900	0.998	7400	0.865
3250	0.398	4100	1.000	5200	0.986	6000	1.000	7500	0.960
3300	0.522	4200	1.000	5300	1.000	6100	0.974	7600	1.000
3350	0.636	4300	0.957	5400	0.955	6200	0.940	7700	0.998
3400	0.735	4400	0.895	5500	0.865	6300	0.901	7800	0.985
3450	0.813	4500	0.802	5600	0.750	6400	0.859	7900	0.973

Table 1 is published in its entirety in the electronic edition of the *PASP*. A portion is shown here for guidance regarding its form and content.

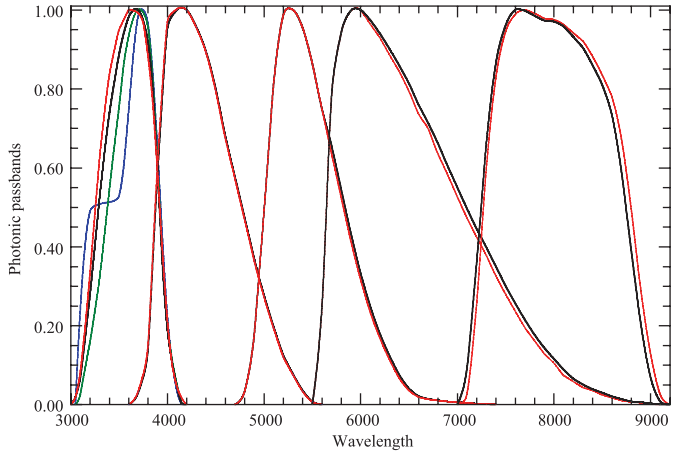

FIG. 9.—Photonic passbands (system response functions) $S_x(\lambda)$ for $UBVRI$. This article—thick line, U: Maiz Appellaniz (2006)—dark-gray line with kink; $U3$: Buser & Kurucz (1978)—dark-gray line, and Bessell (1990a)—light-gray line (see text for details). See the electronic edition of the *PASP* for a color version of this figure.

5.3. The *R* and *I* Passbands

It was not as straightforward to check the R and I bands because of the lack of precise RI photometry for many of the NGSL and MILES stars. The $V-I$ colors given in the *Hipparcos* Catalogue are of uncertain heritage, as are similar data from SIMBAD. An homogenized VRI catalog would have been very useful. Our observational data comprised the *Hipparcos* $V-I$ color supplemented with VRI data mostly from Bessell (1990b) and Koen et al. (2010) for the K and M dwarfs. Although the scatter was high for the *Hipparcos* $V-I$ comparison, it did indicate that a small shift in the Bessell (1990a) $I90$ band was needed. We eventually shifted the red edge of the $R90$ band a little redward and the whole $I90$ band a little blueward. In addition to the synthetic photometry from the NGSL and MILES samples, we also had available a small sample of unpublished single observations of mostly late-type M dwarfs taken with the double-beam spectrograph (DBS) at Siding Spring Observatory. As shown in Figure 7, the resultant synthetic $V-R$ versus $V-I$ relations were in excellent agreement with the empirical loci defined by the precise values in Menzies et al. (1989), Menzies (1990, private communication), Landolt (2009), Bessell (1990b), and Koen et al. (2010). The four empirical data sets are essentially coincident. The sparse redder loci in the $V-R$ versus $V-I$ diagram beyond $V-I\sim1.8$ are Landolt K and M giants. Note that this and later figures are best viewed magnified in the electronic version.

To better appreciate the comparison, we fitted a ninth-order polynomial to the empirical $V-R$ versus $V-I$ locus and plotted the $V-R$ residuals of the fit against $V-I$. Applying the same polynomial, we also computed $V-R$ residuals for the synthetic photometry. In Figure 8 we overlay the synthetic residuals, which are seen to agree very well with the trends in the empirical residuals. The few hundredths-of-a-magnitude systematic differences between the MILES VRI colors for the M dwarfs compared with the empirical stars is undoubtedly

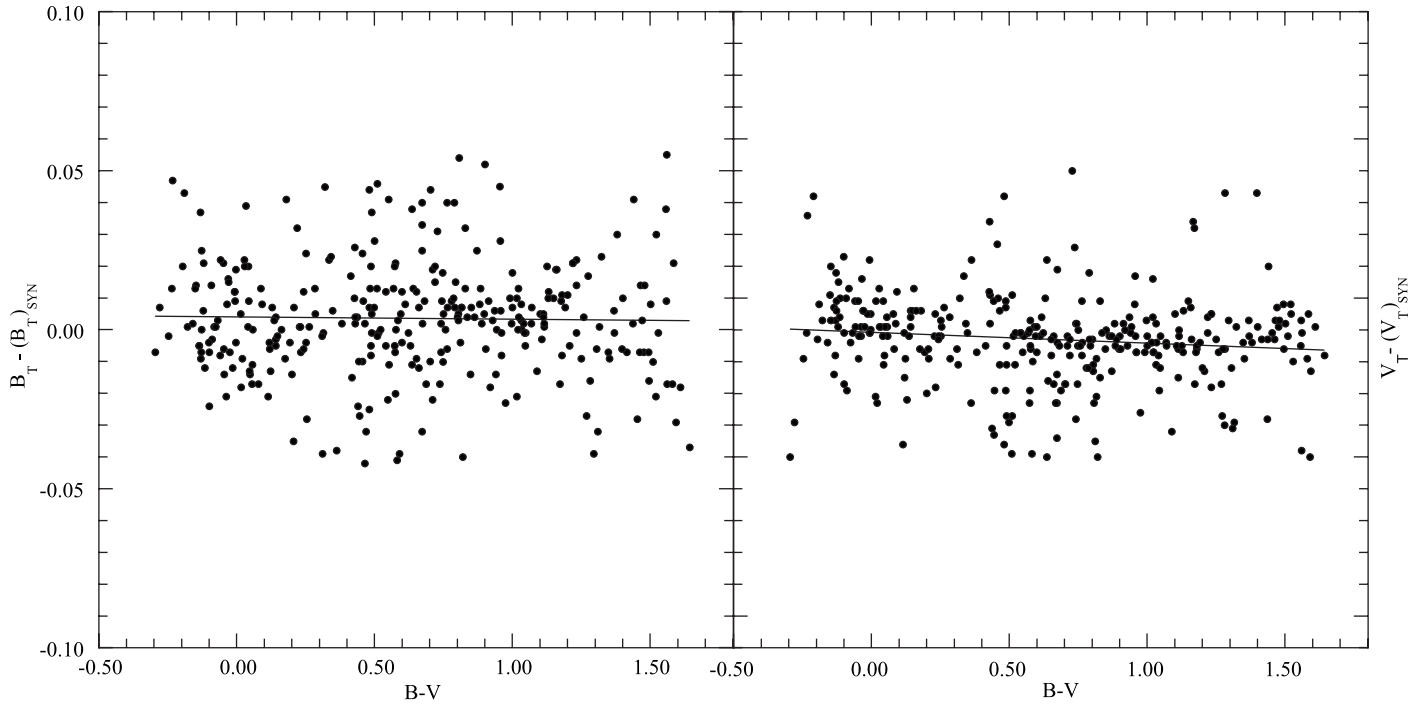

FIG. 10.—Differences between synthetic B_T and V_T and catalog B_T and V_T for the NGSL sample of stars.

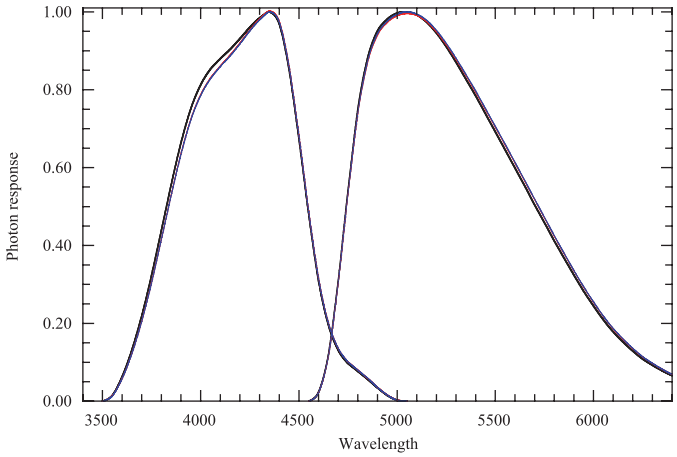

FIG. 11.—Photon-counting response functions $S_x(\lambda)$ for B_T and V_T. This article—thick line, van Leeuwen et al. (1997a)—dark-gray line, and Bessell (1990a)—light-gray line. See the electronic edition of the *PASP* for a color version of this figure.

due to the extrapolation of the MILES spectra from 7000 Å to 9900 Å using model spectra. However, for non-M stars, the relation defined by the extrapolated MILES spectra is indistinguishable from the others, indicating an impressive fidelity of the ATLAS (Munari et al. 2005) and MARCS (Gustafsson et al. 2008) spectra.

5.4. Photometric Passbands: Photon-counting and Energy-integrating Response Functions

There continues to be some confusion in the definition of photometric response functions and their use in computing synthetic photometry. As discussed in Koornneef et al. (1986), Bessell et al. (Appendix 4, 1998), and Maiz Appellaniz (Appendix A, 2006), in the era before CCDs, photometry was largely done with energy-measuring detectors. The normalized response functions, $S'_x(\lambda)$, that were generally published described the relative fraction of energy detected at different

TABLE 2

NORMALIZED H_p B_T, AND V_T PHOTONIC RESPONSES

Wave		H_p	Wave	B_T	Wave	V_T
3400	.....	0.000	3500	0.000	4550	0.000
3500	.....	0.041	3550	0.015	4600	0.023
3600	.....	0.072	3600	0.063	4650	0.119
3700	.....	0.133	3650	0.132	4700	0.308
3800	.....	0.199	3700	0.220	4750	0.540
3900	.....	0.263	3750	0.323	4800	0.749
4000	.....	0.347	3800	0.439	4850	0.882
4100	.....	0.423	3850	0.556	4900	0.951
4200	.....	0.508	3900	0.664	4950	0.981
4300	.....	0.612	3950	0.751	5000	0.997

Table 2 is published in its entirety in the electronic edition of the *PASP*. A portion is shown here for guidance regarding its form and content.

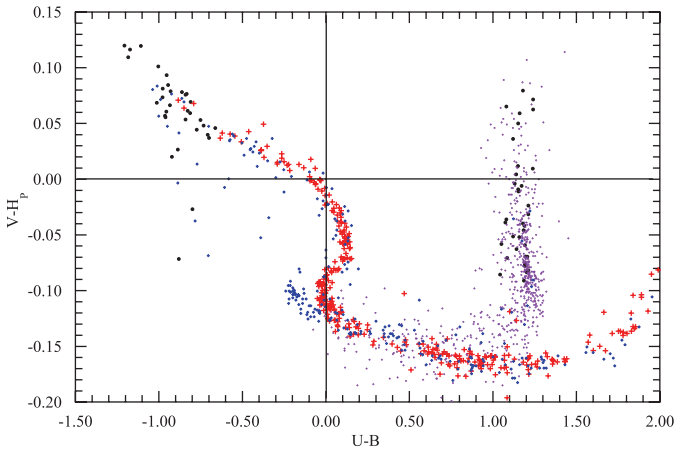

FIG. 12.—Comparison between synthetic and catalog $V - H_P$ vs. $U - B$ relations. Synthetic: NGSL—small plusses. Observed: E-region stars—large plusses, Kilkenny et al. (1998): more extreme O and B stars and M dwarfs—large dots, and Koen et al. (2010): K and M *Hipparcos* dwarfs—light-gray dots. Note the large number of metal-deficient F and G stars in the NGSL sample with $U - B$ excesses and the very few K and M dwarfs in the NGSL sample (see text for details). See the electronic edition of the *PASP* for a color version of this figure.

wavelengths across a particular passband. Nowadays, detectors are almost all photon-integrating devices, such as CCDs, and the response functions used, $S_x(\lambda)$, relate to the relative number of photons detected (or the probability of a photon being detected) at different wavelengths across the passband. These issues are outlined and explored in the Appendix, where it is also shown why the magnitudes derived from photon-counting or energy-integration observations are identical (as expected). In Table 1 we list our adopted normalized photon-counting passbands $S_x(\lambda)$ for U, B, V, R, and I. In Figure 9 we show the

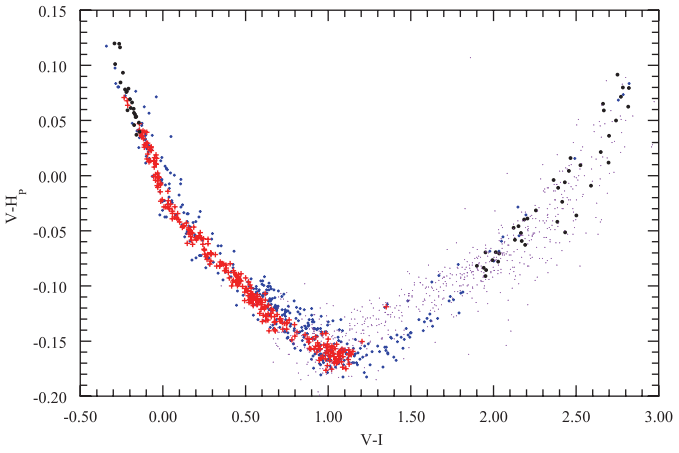

FIG. 13.—Comparison between synthetic and catalog $V - H_P$ vs. $V - I$ relations. Synthetic: NGSL—small plusses. Observed: E-region stars—large plusses, Kilkenny et al. (1998)—large dots, and Koen et al. (2010)—small dots (see text for details). See the electronic edition of the *PASP* for a color version of this figure.

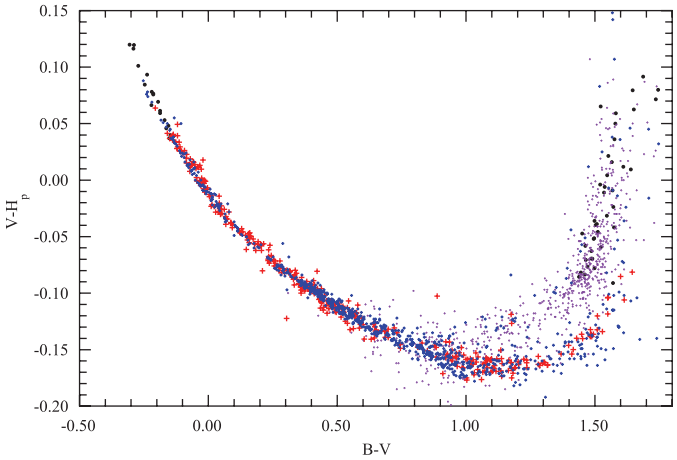

FIG. 14.—Comparison between synthetic and catalog $V - H_P$ vs. $B - V$ relations. Synthetic: NGSL—small plusses. Observed: E-region stars—large plusses, Kilkenny et al. (1998)—large dots, and Koen et al. (2010)—small dots (see text for details). See the electronic edition of the *PASP* for a color version of this figure.

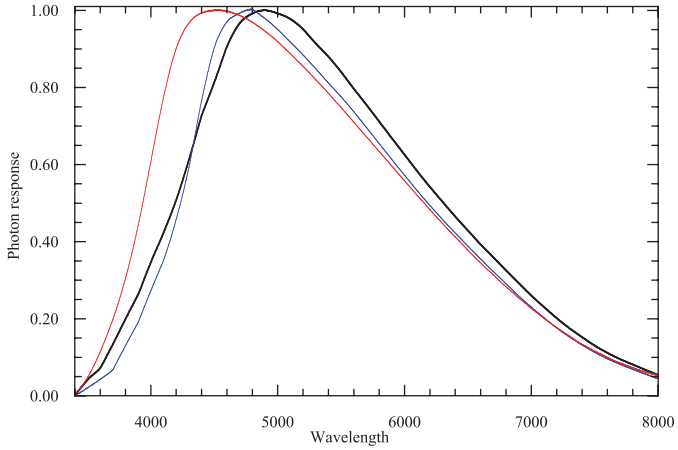

FIG. 16.—Photonic response functions $S(\lambda)$ for H_p. This article—thick line, van Leeuwen et al. (1997a)—light-gray line, and Bessell (1990a)—dark-gray line (see text for details). See the electronic edition of the *PASP* for a color version of this figure.

normalized photon-counting passbands for U, B, V, R, and I compared with the Bessell (1990a) passbands converted to photon-counting. The Maiz Appellaniz (2006) U band and the converted Buser & Kurucz (1978) photon-counting $U3$ band are also shown.

6. *HIPPARCOS* H_p AND TYCHO B_T AND V_T PASSBANDS

There are two ground-based photometric systems notable for their precision and stability. These are the Walraven $VBLUW$ photometry of Pel & Lub (2007) and the $UBVRI$ SAAO and Landolt (2009) photometry discussed previously. Pel (1990, private communication) also provided precise transformations between the Johnson-Cousins V and $B - V$ and Walraven V and $V - B$.

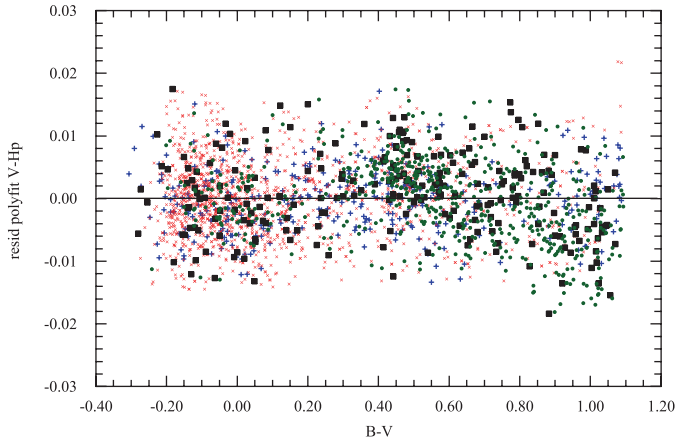

FIG. 15.—Comparison between the residuals of the same polynomial fit to the synthetic and catalog $V - H_P$ vs. $B - V$ relations. Synthetic: NGSL—squares and MILES—dots. Observed: E-region stars Menzies et al. (1989,1990, private communication)—crosses, Pel & Lub (2007) and Pel (1990, private communication)—plusses (see text for details). See the electronic edition of the *PASP* for a color version of this figure.

We regressed $V - H_p$, $B - B_T$, and $V - V_T$ versus $B - V$ for these two data sets and compared them with the synthetic photometry from the NGSL and MILES. As done for UBV, the H_p, B_T, and V_T passbands were adjusted until the slopes and shapes of the regressions with the synthetic photometry matched as closely as possible those of the observed regressions. In order to remove the small color term evident in the initial regressions, the red side of the Bessell (2000) V_T passband was shifted slightly redward, while a smaller blueward shift was made to the blue side of the Bessell (2000) B_T band. Figure 10 shows the final regressions for $B - B_T$ and $V - V_T$ from the NGSL spectra. Figure 11 shows the adopted B_T and V_T passbands in comparison with the original passbands (van Leeuwen et al. 1997a) and the Bessell (2000) passbands. There is little obvious difference between the three passbands. The adopted photon-counting response functions for B_T and V_T are listed in Table 2.

There have been suggestions (e.g., Grenon 2001, private communication), that the change in the H_p sensitivity function caused by the in-orbit radiation damage was unlikely to be a complete loss of the bluest sensitivity as suggested by Bessell (2000), but rather a more complicated drop in sensitivity across a wider wavelength range. We have attempted to use the two spectrophotometric samples to examine this proposition and, although the results are not unequivocal, a slightly better fit is achieved by making small modifications to the Bessell (2000) passband.

The synthetic $V - H_p$ versus $U - B$, $V - I$, and $B - V$ regressions are shown in Figures 12, 13, and 14, respectively,

TABLE 3
$UBVRI$ ZERO POINTS BASED ON STIS005 SPECTRUM AND $V = 0.03$ FOR VEGA

System	U	B	V	R	I	B_T	V_T	H_p
AB_ν = abmag	0.771	−0.138	−0.023	0.160	0.402	−0.090	−0.044	−0.022
AB_λ = stmag	−0.142	−0.625	−0.019	0.538	1.220	−0.672	−0.115	−0.074
vegamag	−0.023	−0.023	−0.023	−0.023	−0.023	−0.023	−0.023	−0.023
$\lambda_{\rm eff}$	3673	4368	5455	6426	7939	4215	5265	5188

in comparison with empirical relations for these stars. These plots show the range of stars represented in the NGSL spectrophotometric catalog (few K and M dwarfs, but many FG subdwarfs) and the different distribution of stars in the comparison standard photometric SAAO catalogs. We have fitted a cubic polynomial to the $V - H_p$ versus $B - V$ regression for the E-region stars (Menzies et al. 1989; Menzies 1990, private communication) bluer than $B - V = 1.1$. The same polynomial in $B - V$ was applied to the catalog stars of Pel & Lub (2007) and Pel (1990, private communication) and to the synthetic photometry of the NGSL and MILES stars.

In Figure 15 we plot the residuals of the fit. It is clear that the synthetic photometry using the adopted H_p band is a very good match to the standard photometry, with the caveat that the ZPs of the synthetic $V - H_p$ magnitudes were adjusted to achieve this. This will be discussed in the next section. Table 2 also lists the new *Hipparcos* passband, and Figure 16 shows the new and old photon-counting passbands.

7. *UBVRI*, H_p, B_T, AND V_T MAGNITUDES AND ZERO POINTS

All standard photometric systems adopt some ZP for their magnitude scale. Historically, the ZP of V in the UBV system is generally used for other systems.

The AB-magnitude system (Oke & Gunn 1983; also see the Appendix) was defined as a monochromatic-magnitude system for spectrophotometry, where $AB_\nu = -2.5 \log f_\nu + 48.60$, and f_ν is the flux in erg cm^{-2} s^{-1} Hz^{-1}. This has now been generalized for use with broadband photometric bands. In the AB system, a flat-spectrum star (in f_ν) has the same AB magnitude in all passbands.

The AB_λ- or ST-magnitude system (see the Appendix) was defined in terms of f_λ, where $ST = -2.5 \log f_\lambda + 21.10$

The so-called VEGAMAG system (like the UBV system) is one where Vega (α Lyrae) has colors (magnitude differences), such as $U - B$ and $B - V$, that are identically zero. This is equivalent to dividing all the observed fluxes by the flux of Vega but adjusting the V ZP to give the adopted V magnitude for Vega. For the Vega spectrum we used the CALSPEC[5] spectrum alpha_lyr_stis_005, which is distributed in the synphot and pysynphot software packages (see the Appendix).

[5] See http://www.stsci.edu/hst/observatory/cdbs/calspec.html.

7.1. Observed Zero Points

The *Hipparcos*- and Tycho-magnitude ZPs (van Leeuwen et al. 1997b) were chosen to produce a VEGAMAG-type system in which $H_p = V_T = V$ and $B_T = B$ at $B - V = 0$, where B and V are standard magnitudes in the Johnson-Cousins UBV system. Pel & Lub (2007) confirmed the excellent agreement between the V-magnitude scales of the homogenized UBV system (Nicolet 1978), the $uvby$ system (Gronbech & Olsen 1976; Olsen 1983), the *Hipparcos* system, and the Walraven V and $V - B$ system [Pel 1990, private communication; transformed with $V_{\rm PL} = 6.886 - 2.5V_W - 0.080(V_W - B_W)$].

We have intercompared the Pel & Lub (2007) transformed $V_{\rm PL}$ magnitudes with those from the *Hipparcos* Catalogue (Perryman et al. 1997), the most recent homogenized UBV catalog,[6] and the E-region photometry from Menzies et al. (1989) and Menzies (1990, private communication). [We also derived $B - V = 2.539(V_W - B_W) - 0.827(V_W - B_W)^2 + 0.3121(V_W - B_W)^3 - 0.015$ from 1654 common stars in the homogenized UBV catalog.[7] The transformed $B - V$ values had an rms of 0.013 mag. A slightly different fit was obtained using SIMBAD $B - V$ values.] The results of the V comparisons were $V_{\rm Hip} = V_{\rm PL} - 0.006$ (1523 stars) and $V_{\rm Merm} = V_{\rm PL} - 0.005$ (1679 stars); the rms values of these means are 0.0003 mag. The ZP differences are similar to the $V_{\rm SAAO} \approx V_{\rm PL} - 0.006$ reported by Cousins & Menzies (1993). We derived $V - H_p$ for the various observed samples and by fitting a cubic to the regressions against $B - V$ for $-0.3 < B - V < 1.1$ have determined the $V - H_p$ values for $B - V = 0$. These are -0.008 (358 E-region stars), -0.009 (78 Landolt 2009 stars), and -0.0003 (1427 Pel & Lub 2007 stars). We also derived $V - V_T$ and $B - B_T$ and fitted polynomials to the $B - V$ regressions, yielding $V - V_T$ ZPs of $+0.002$ (355 E-region stars) $+0.008$ (1618 Pel & Lub 2007 stars) and $B - B_T$ ZPs of -0.003 (367 E-region stars) and $+0.002$ (1708 Pel & Lub 2007 stars).

From these comparisons we confirm that Menzies et al. (1989), Menzies (1990, private communication), Landolt (2009), and Mermilliod[8] have the same V-magnitude ZP and that the transformed $V_{\rm PL}$ magnitudes (Pel 1990, private communication) should be adjusted by -0.006 mag. (The original

[6] Vizier Online Data Catalog, II/168 (J. C. Mermilliod, 2006).
[7] Vizier Online Data Catalog, II/168 (J. C. Mermilliod, 2006).
[8] Vizier Online Data Catalog, II/168 (J. C. Mermilliod, 2006).

TABLE 4
MEAN DIFFERENCES BETWEEN THE SYNTHETIC AND OBSERVED PHOTOMETRY

Source	V	$U-B$	$B-V$	$V-R$	$V-I$	B_T	V_T	$V-H_p$	$N_{\rm stars}$
NGSL	0.002	−0.018	0.005	∼0.0	0.004	−0.010	0.007	0.012	∼300
MILES	0.004	...	−0.012	∼0.0	−0.006	−0.032	0.007	0.012	∼700

Walraven $VBLUW$ magnitudes are unaffected.) Although the ZPs of the H_p, V_T, and B_T systems need to be adjusted by -0.008, $+0.002$, and -0.003 mag, respectively, to put them on the same ZP as the $UBVRI$ system, we will retain the ZPs of the existing H_p, B_T, and V_T systems defined by the *Hipparcos* and Tycho catalogs in this article and derive synthetic photometry ZP corrections accordingly.

7.2. Synthetic Photometry Zero Points

We carried out synthetic photometry on the Vega STIS005 (alpha_lyr_stis_005) spectrum and assigned ZPs to force $H_p = V_T = B_T = U = B = 0.03$ (see the Appendix). These Vega-based f_ν and f_λ ZPs are listed in Table 3. All ZPs in this article are to be subtracted from the AB magnitudes (eq. [1]).

With these ZPs we computed synthetic photometry for all NGSL and MILES stars that had *Hipparcos* photometry. The ZPs from the synthetic photometry will check (1) whether there are systematic differences between the mean MILES and NGSL flux calibrations and (2) whether the STIS005 spectrum correctly represents the empirical ZPs of the $UBVRI$ and H_p, V_T, and B_T systems. We compared the synthetic magnitudes and/or colors with the observed magnitudes and colors and derived the mean differences. The few stars with exceptionally large differences were not used in the means. There were about 700 stars in the MILES sample and 300 stars in the NGSL sample. We also computed synthetic photometry for 46 of the CALSPEC spectra,[9] 27 of which have $UBVRI$ photometry from Landolt & Uomoto (2007) and Landolt (2009), 16 had H_p photometry, and 10 had Tycho photometry.

In Table 4 we list the mean differences. The standard errors of the means for the NGSL and MILES samples are less than 0.001 mag. There was good agreement between the NGSL and MILES VRI, V_T, and H_p results; however, the differences for B and B_T appear to be small but real. We chose to adopt the NGSL values for B and B_T in preference to the MILES values, as the NGSL data were taken outside the atmosphere and are unaffected by atmospheric extinction. For the far fewer CALSPEC spectra, the errors in the mean were between 0.004 (H_p) and 0.04 (B_T and V_T). Given the small number of CALSPEC stars with photometry, the mean differences in the colors of the much fainter CALSPEC spectra were in reasonable agreement with those for the NGSL sample, except for an unexplained difference of a few hundredths of a magnitude between the V and H_p magnitudes.

In Table 5 we list the additional ZP-magnitude offsets that will place synthetic photometry computed with the AB-magnitude ZPs from Table 3 on the same scale as the homogeneous UBV system, the Cousins-Landolt $UBVRI$ system, and the *Hipparcos* and Tycho systems. We also list two wavelengths associated with each passband, which are defined independently of the flux: the pivot wavelength λ_p and the mean photon wavelength λ_0 (see the Appendix for details) and the FWHM of the passband; the wavelengths are given in angstroms. Note that these are the wavelengths that should be associated with published $UBVRI$ photometry, not the natural passbands used by various observers, as their photometry has been transformed onto the standard system. The uncertainties in these additional zero points should only be a few millimagnitudes, except for R and I, where it is more uncertain, as the available $V-I$ photometry was of lower precision. Using these total ZP corrections we recomputed the magnitudes for the Vega stis005 spectrum and obtained $V = 0.027$, $U-B = 0.018$, $B-V = -0.004$, $V-R = 0.000$, and $V-I = -0.001$. In addition, the 1994 ATLAS Vega spectrum of Castelli[10] gives $U-B = -0.017$, $B-V = -0.017$, $V-R = -0.004$, and $V-I = -0.009$. For comparison, Bessell (1983) measured for Vega, $B-V = -0.01$, $V-R = -0.009$, and $V-I = -0.005$.

8. SUMMARY

Excellent spectrophotometric catalogs are now available from NGSL[11] (Heap & Lindler 2007) and MILES[12] (Sanchez-Blazquez et al. 2006). In addition to their intrinsic worth, such stars are very useful to use to calibrate all-sky surveys, such as SkyMapper (Keller et al. 2007). However, the published absolute flux levels are imprecise or nonexistent, so we have renormalized the spectra to their precise H_p magnitudes. In order to do this it was necessary to determine the best H_p passband. We also decided to reexamine the passbands representing the $UBVRI$ and Tycho B_T and V_T standard photometric systems using the renormalized NGSL and MILES spectra. We used the CALSPEC stis005 spectrum of Vega to derive the nominal ZP corrections to the AB-magnitude fluxes and synthesized the various magnitudes and slightly adjusted the photonic passbands,

[9] See http://www.stsci.edu/hst/observatory/cdbs/calspec.html.

[10] See http://wwwuser.oat.ts.astro.it/castelli/vega/fm05t9550g395k2odfnew.dat.

[11] See http://archive.stsci.edu/prepds/stisngsl/index.html.

[12] See http://www.iac.es/proyecto/miles/.

TABLE 5
ADOPTED ADDITIONAL ZP MAGNITUDES AND PASSBAND PARAMETERS

	U	B	V	R	I	B_T	V_T	H_p
ZP	−0.010	0.008	0.003	0.003	0.002	−0.010	0.007	−0.008
$\Delta\lambda_{fwhm}$	625	890	830	1443	1499	718	962	2116
λ_p	3597	4377	5488	6515	7981	4190	5300	5347
λ_0	3603	4341	5499	6543	7994	4198	5315	5427

NOTES.—These zero points are to be applied in addition to those in Table 3 based on the STIS005 spectrum of Vega. See § A2.1 for the definition of other wavelengths associated with passbands.

achieving better agreement between the synthetic and standard magnitudes than was possible with the previous passbands. In Tables 3 and 4 we present the adopted photonic passbands for $UBVRI$ and H_p, B_T, and V_T, respectively. Table 5 lists the ZP-magnitude corrections based on the stis005 Vega spectrum and $V = 0.03$.

We intercompared the ZPs of the V-magnitude scale of the SAAO Cousins-Landolt $UBVRI$ system, the homogenized UBV system,[13], the Walraven Pel & Lub (2007) system, and the *Hipparcos* H_p and Tycho B_T and V_T systems. We found small differences of less than 0.01 mag between them. The H_p-magnitude ZP differs by 0.008 mag from the ZP of the $UBVRI$ system.

We analyzed the mean magnitude and color differences between the synthetic photometry and the standard photometry and proposed small additional ZP corrections to place the synthetic photometry computed using the AB-magnitude ZPs in Table 5 onto the same ZPs as the standard system photometry. These additional ZP corrections are given in Table 3, together with the passband parameters that should be used to characterize the standard systems.

There was good agreement between the mean differences from the NGSL and MILES catalogs, although the mean level of the MILES blue fluxes deviated slightly, but systematically, from those of the NGSL spectra. The synthetic colors of the fainter CALSPEC spectra also support the proposed additional ZP corrections, except for an unexplained difference in the relative V and H_p magnitudes.

Finally, in the Appendix, we present an extensive discussion on the confusion in the literature concerning measured magnitudes, fluxes, and response functions when broadband photometry is involved, and we provide equations that clearly set out the derivation of photometric quantities. We also cross-reference parameters and definitions used in the *Hubble Space Telescope* photometric packages synphot and its successor pysynphot (§ A2.3).

We wish to thank Sally Heap for correspondence concerning the rereduction of the Next Generation Spectral Library (NGSL) spectra, Jan Willem Pel and Jan Lub for a digital version of their Walraven photometry catalog and for helpful discussions, and Wolfgang Kerzendorf for fitting and extrapolating the Medium Resolution INT Library of Empirical Spectra (MILES) spectra to cover the 3000 Å–1,200 Å wavelength region. We thank the referee for suggestions to make the article more accessible to physicists. VizieR, Simbad, TOPCAT, and Kaleidagraph were used in preparing this article.

A.
APPENDIX

Unfortunately, there is some confusion in the literature concerning measured magnitudes, fluxes, and response functions when broadband photometry is discussed. The definitions concerning monochromatic fluxes are clear—but see Soffer & Lynch (1999) concerning the paradoxes, errors, and confusions that arise when density distributions are involved—but the clarity is lost when these definitions are generalized to involve mean magnitudes, mean fluxes, and the choice of the "effective" wavelength or frequency most appropriately associated with them.

A1. Photometric Quantities and Definitions

In astronomy, flux (f) refers to the radiative flux density, a quantity in physics referred to as the spectral irradiance. In astronomy, flux is also referred to as the monochromatic flux f_ν or f_λ, to distinguish it from the total flux F, which is summed over all wavelengths or frequencies. In SI units, f_λ is measured in $\mathrm{W\,m^{-3}}$ or, more practically, in $\mathrm{W\,m^{-2}\,\text{Å}^{-1}}$, $\mathrm{W\,m^{-2}\,nm^{-1}}$, or $\mathrm{W\,m^{-2}\,\mu m^{-1}}$, depending on the part of the spectrum being considered. In cgs units it is measured in $\mathrm{erg\,cm^{-2}\,s^{-1}\,\text{Å}^{-1}}$, $\mathrm{erg\,cm^{-2}\,s^{-1}\,nm^{-1}}$ or $\mathrm{erg\,cm^{-2}\,s^{-1}\,\mu m^{-1}}$. ($10^3$ $\mathrm{erg\,cm^{-2}\,s^{-1}} = 1$ $\mathrm{W\,m^{-2}}$). In radio astronomy, fluxes are usually expressed in terms of a non-SI unit, the flux unit or jansky (Jy), which is equivalent to 10^{-26} $\mathrm{W\,m^{-2}\,Hz^{-1}}$ or 10^{-23} $\mathrm{erg\,cm^{-2}\,s^{-1}\,Hz^{-1}}$.

[13] Vizier Online Data Catalog, II/168 (J. C. Mermilliod, 2006).

A good starting point for the relevant formulae and definitions used in photometry is Rufener & Nicolet (1988), Koornneef et al. (1986), and Tokunaga & Vacca (2005). The stellar flux is normally given in terms of f_ν or f_λ, and the units, respectively, are erg cm^{-2} s^{-1} Hz^{-1} and erg cm^{-2} s^{-1} Å^{-1} or, in the SI system of units, W m^{-2} Hz^{-1} and W m^{-2} nm^{-1}; although, rather than energy, the photon flux n_p in photon m^{-2} s^{-1} Hz^{-1} or photon m^{-2} s^{-1} Å^{-1} is also used. The relations between these quantities are precisely defined for monochromatic light: namely,

$$f_\nu = f_\lambda \frac{\lambda^2}{c} \tag{A1}$$

and

$$n_p = f_\lambda \frac{\lambda}{hc}. \tag{A2}$$

The AB (absolute) magnitude scale was introduced by Oke (1965), who proposed the f_ν definition, having noted that a plot of f_ν versus $1/\lambda$ for hot stars, was approximately linear in the optical part of the spectrum. The monochromatic-magnitude AB was later defined by Oke & Gunn (1983) using the flux measurement adopted by Oke & Schild (1970) for Vega at 5480 Å and an apparent magnitude of $V = +0.035$. The Vega flux was considered measured to an accuracy of about 2%. Oke & Schild (1970) measured the flux of Vega at a set of discrete 50 Å bands. A mean value of $f_\nu = 3.46 \times 10^{-20}$ erg cm^{-2} s^{-1} Hz^{-1} or 3.36×10^{-9} erg cm^{-2} s^{-1} Å^{-1} or 940 photon cm^{-2} s^{-1} Å^{-1} was measured at 5556 Å. They then interpolated Vega's flux to the value of 3.65×10^{-20} erg cm^{-2} s^{-1} Hz^{-1} at 5480 Å, assumed to be the "effective" wavelength of the V band, and using this value together with $V = +0.035$, they derived the constant -48.60 associated with definition for the AB magnitude: namely,

$$\mathrm{AB}_\nu = -2.5 \log f_\nu - 48.60. \tag{A3}$$

It is somewhat unfortunate that Oke (1965) chose to define the AB magnitude in terms of f_ν rather than f_λ, which is more appropriate for most stars—but the conversions, at least for monochromatic light, are straightforward:

$$\mathrm{AB}_\lambda = -2.5 \log f_\lambda - 21.10. \tag{A4}$$

AB_λ is called STMAG in synphot and pysynphot. Note that these ZPs are based on the nominal wavelength of 5480 Å for the V band.

More recent measurements of Vega's flux are about 2% brighter, and retaining the preceding values of the ZPs in the definition of AB magnitude and ST magnitude will mean that these scales will necessarily have different ZPs from the V system. And if a different nominal wavelength for the V band is adopted, this will introduce an additional systematic difference between the f_ν and f_λ ZPs.

A1.1. The Flux and *V* Magnitude of Vega

Summaries of the direct measurements of the optical flux of Vega are given by Hayes (1985) and Megessier (1995), who proposed $f_\lambda = 3.44 \pm 0.05 \times 10^{-9}$ and $3.46 \pm 0.01\times 10^{-9}$ erg cm^{-2} s^{-1} Å^{-1}, respectively, for Vega at 5556 Å. Cohen et al. (1992) adopted the Hayes value, together with the flux spectrum of a Vega ATLAS 9 model for their spectral irradiance calibration. More recently, Bohlin & Gilliland (2004) measured the flux for Vega using STIS spectra, and Bohlin (2007) refined these observations and discussed model fits, including rapidly rotating pole-on models. Bohlin (2007) quoted an absolute flux at 5556 Å, the same as Megessier (1995), and $V = 0.023$ and adopted for Vega a combination of various source fluxes to produce the CALSPEC spectrum alpha_lyr_stis_005 that is now generally used by pysynphot and other routines.

Many direct V measurements of Vega have been made over the years. An obvious problem has been its extreme brightness, making it difficult to measure with sensitive photomultipliers on 1 m telescopes; however, Bessell (1983) measured $V = 0.03$ in comparison with Cousins bright equatorial stars using an Inconel-coated 1% neutral density filter and a GaAs photomultiplier tube at Kitt Peak. This value is in exact agreement with Johnson et al. (1966). Hayes (1985) discussed measurements of the V magnitude of Vega and discounted reports of its variability. More recently, Gray (2007) also discussed observations of Vega. Mermilliod[14] gave $V = 0.033 \pm 0.012$ for Vega.

We have computed $V = 0.007$ from the CALSPEC spectrum of Vega using our passband and the ZP of -48.60 in equation (A3). This implies that ZPs of -48.58 and -21.08, respectively, would put the AB_ν and AB_λ-magnitude scale on the same ZP as the V-magnitude system, but see § 7.2.

A2. Issues Arising from a Broad Passband

Photometric observations are normally made by summing the flux over discrete wavelength intervals defined by a window (filter) function. A generalized filter function is a dimensionless (unitless) quantity R representing the fraction of the flux f at each wavelength, which is incident on the detector. It is the product of the atmospheric transmission, the mirror reflectivity, the optics transmission, and the glass filter transmission. It is usually used in the form of a normalized function. The mean f_λ flux would be expressed by the following equation:

$$\langle f_\lambda \rangle = \frac{\int f_\lambda(\lambda) R(\lambda) d\lambda}{\int R(\lambda) d\lambda}, \tag{A5}$$

and a similar equation for $\langle f_\nu \rangle$ with all λ replaced by ν. All integrals are nominally from zero to infinity, but are sensibly evaluated over the defined range of the filter passband.

[14] Vizier Online Data Catalog, II/168 (J. C. Mermilliod, 2006).

One source of confusion is the fact that the flux is evaluated after the detector, not before it. This means that the filter function must be multiplied by the response function of the detector to give the system response function, as the detector converts the incident light into electrons, which are then amplified and measured. In the case of a photon-counting detector, such as a CCD, the function R is multiplied by the quantum efficiency $\eta(\lambda)$ of the CCD to give the system photon response function S. In the case of detectors with photocathodes using DC techniques and current integration, the function R is multiplied by the photocathode radiant response $\sigma(\lambda)$ (in units of mA/W) to give the system energy response function S'. Incorrect equations for photon-counting and energy integration (e.g., Buser 1986, eqs. [1] and [2]) result from overlooking this difference. The system response functions are then generally renormalized.

The relations between $S(\lambda)$, $S'(\lambda)$, $\eta(\lambda)$, and $\sigma(\lambda)$ are

$$S(\lambda) = R(\lambda)\eta(\lambda) \qquad S'(\lambda) = R(\lambda)\sigma(\lambda) \tag{A6}$$

$$\eta(\lambda) = \frac{hc}{e\lambda}\sigma(\lambda) = \frac{12.4}{\lambda}\sigma(\lambda), \tag{A7}$$

where λ is in angstroms, η is in percent, and σ is in mA W^{-1}, or in frequency units,

$$\eta(\nu) = \frac{h\nu}{e}\sigma_\nu(\nu). \tag{A8}$$

Ignoring the atomic constants for the moment (and noting that the response functions are usually normalized), we can write

$$S'(\lambda) = R(\lambda)\eta(\lambda)\lambda = S(\lambda)\lambda \tag{A9}$$

and

$$S'(\nu) = R(\nu)\eta(\nu)/\nu = S(\nu)/\nu. \tag{A10}$$

So for an energy-integrating detector we can express the measured mean energy flux as

$$\langle f_\lambda\rangle = \frac{\int f_\lambda(\lambda)S'(\lambda)d\lambda}{\int S'(\lambda)d\lambda} = \frac{\int f_\lambda(\lambda)S(\lambda)\lambda d\lambda}{\int S(\lambda)\lambda d\lambda}, \tag{A11}$$

and for $\langle f_\nu\rangle$,

$$\begin{aligned}\langle f_\nu\rangle &= \frac{\int f_\nu(\nu)S'(\nu)d\nu}{\int S'(\nu)d\nu} = \frac{\int f_\nu(\nu)S(\nu)d\nu/\nu}{\int S(\nu)d\nu/\nu} \\ &= \frac{\int f_\lambda(\lambda)(\lambda^2/c)S(\lambda)\lambda\frac{c}{\lambda^2}d\lambda}{\int S(\lambda)\lambda(c/\lambda^2)d\lambda} = \frac{\int f_\lambda(\lambda)S(\lambda)\lambda d\lambda}{\int S(\lambda)(c/\lambda)d\lambda}.\end{aligned} \tag{A12}$$

For photon-counting detectors, one electron is collected for every detected photon, so the mean photon flux is given by

$$\begin{aligned}\langle n_p\rangle &= \frac{\int n_p(\lambda)S(\lambda)d\lambda}{\int S(\lambda)d\lambda} \\ &= \frac{\int f_\lambda(\lambda)(\lambda/hc)S(\lambda)d\lambda}{\int(\lambda/hc)S(\lambda)d\lambda} \times \frac{\int S(\lambda)(\lambda/hc)d\lambda}{\int S(\lambda)d\lambda} = \langle f_\lambda\rangle\frac{\lambda_0}{hc},\end{aligned} \tag{A13}$$

where

$$\lambda_0 = \frac{\int \lambda S(\lambda)d\lambda}{\int S(\lambda)d\lambda}. \tag{A14}$$

Equation (A13) is very important because it shows that in broadband photometry, the mean photon flux is proportional to the mean energy flux and counting photons is equivalent to integrating the energy. Furthermore, the wavelength λ_0 is the representative wavelength of the mean photons and could be called the mean photon wavelength of the passband.

A2.1. Definitions of Other Wavelengths and Frequencies Associated with a Passband

Now, because monochromatically $f_\nu = f\lambda(\lambda^2/c)$, we can write that

$$\langle f_\nu\rangle = \langle f_\lambda\rangle\frac{\lambda_p^2}{c}, \tag{A15}$$

where λ_p is called the pivot wavelength and from equations (A11) and (A12) can be shown to be

$$\lambda_p = \sqrt{\frac{\int S(\lambda)\lambda d\lambda}{\int \frac{S(\lambda)}{\lambda}d\lambda}}. \tag{A16}$$

As noted by Koornneef et al. (1986), the pivot wavelength is convenient because it allows an exact conversion between the mean broadband fluxes $\langle f_\nu\rangle$ and $\langle f_\lambda\rangle$.

We previously defined the mean photon wavelength λ_0; we could also define the mean energy wavelength: that is,

$$\lambda_0' = \frac{\int \lambda S'(\lambda)d\lambda}{\int S'(\lambda)d\lambda} = \frac{\int S(\lambda)\lambda^2 d\lambda}{\int S(\lambda)\lambda d\lambda}. \tag{A17}$$

This mean wavelength was discussed by King (1952), who cites it as being favored as a flux-independent "effective" wavelength for broadband systems. Two other wavelengths are commonly used: the isophotal wavelength and the effective wavelength.

The isophotal wavelength $\lambda_{\rm iso}$, recommended by Cohen et al. (1992), is the wavelength at which the interpolated, smoothed monochromatic flux has the same value as the mean flux integrated across the band. That is,

$$f_\lambda(\lambda_{\rm iso}) = \langle f_\lambda\rangle = \frac{\int f_\lambda(\lambda)S'(\lambda)d\lambda}{\int S'(\lambda)d\lambda} = \frac{\int f_\lambda(\lambda)S(\lambda)\lambda d\lambda}{\int S(\lambda)\lambda d\lambda}. \tag{A18}$$

A similar expression can be written for the isophotal frequency:

$$f_\nu(\nu_{\rm iso}) = \langle f_\nu \rangle = \frac{\int f_\nu(\nu) S(\nu)/\nu d\nu}{\int S(\nu)/\nu d\nu}. \quad \text{(A19)}$$

Note that both definitions relate to the energy flux, but a different pair of equations could be defined in terms of the photon flux:

$$n_p(\lambda_{\rm iso}) = \langle n_p \rangle = \frac{\int n_p(\lambda) S(\lambda) d\lambda}{\int S(\lambda) d\lambda} = \frac{(1/hc)\int f_\lambda(\lambda) S(\lambda)\lambda d\lambda}{\int S(\lambda)\lambda d\lambda} \times \frac{\int S(\lambda)\lambda d\lambda}{\int S(\lambda) d\lambda} = \langle f_\lambda \rangle \frac{\lambda_0}{hc}. \quad \text{(A20)}$$

The effective wavelength is usually defined as the flux-weighted mean wavelength. In terms of photons,

$$\lambda_{\rm eff} = \frac{\int \lambda n_p(\lambda) S(\lambda) d\lambda}{\int n_p(\lambda) S(\lambda) d\lambda} = \frac{\int \lambda^2 f_\lambda(\lambda) S(\lambda) d\lambda}{\int \lambda f_\lambda(\lambda) S(\lambda) d\lambda}, \quad \text{(A21)}$$

which is the same in terms of energy:

$$\lambda'_{\rm eff} = \frac{\int \lambda f_\lambda(\lambda) S'(\lambda) d\lambda}{\int f_\lambda(\lambda) S'(\lambda) d\lambda} = \frac{\int \lambda^2 f_\lambda(\lambda) S(\lambda) d\lambda}{\int f_\lambda(\lambda) S(\lambda)\lambda d\lambda} \quad \text{(A22)}$$

and

$$\nu'_{\rm eff} = \frac{\int \nu f_\nu(\nu) S'(\nu) d\nu}{\int f_\nu(\nu) S'(\nu) d\nu} = \frac{\int f_\nu(\nu) S(\nu) d\nu}{\int f_\nu(\nu) S(\nu) d\nu/\nu}. \quad \text{(A23)}$$

Note that $\lambda_{\rm iso}$ and $\lambda_{\rm eff}$ depend explicitly on the underlying flux distribution through the filter.

The definitions and labels of the various wavelengths and frequencies have long stirred passions. King (1952) argued strongly against the currently accepted use of "effective wavelength" and "effective frequency" as defined in equations (A22) and (A23), noting that the meaning of "effective wavelength" is better served by the isophotal wavelength. He further proposed that the mean wavelengths, defined in equations (A14) and (A17) to a first approximation, act as effective wavelengths for all stars, being independent of the flux distribution.

Finally, for aesthetic reasons, Schneider et al. (1983) defined the effective frequency for a passband to be

$$\nu^*_{\rm eff} = \exp \langle \ln \nu \rangle = \exp \frac{\int (\ln \nu) n_p(\nu) S(\nu) d\nu}{\int n_p(\nu) S(\nu) d\nu}, \quad \text{(A24)}$$

and it follows that

$$\lambda^*_{\rm eff} = \exp \langle \ln \lambda \rangle = \exp \frac{\int (\ln \lambda) n_p(\nu) S(\nu) d\nu}{\int n_p(\nu) S(\nu) d\nu} = \exp \frac{\int (\ln \lambda) f_\nu(\nu) S(\nu) (1/\nu) d\nu}{\int f_\nu(\nu) S(\nu) (1/\nu) d\nu} = \exp \frac{\int (\ln \lambda) f_\nu(\nu) S(\nu) d(\ln \nu)}{\int f_\nu(\nu) S(\nu) d(\ln \nu)}. \quad \text{(A25)}$$

We note that this is not what Fukugita et al. (1996) claimed Schneider et al. (1983) defined as $\lambda_{\rm eff}$. Fukugita et al. (1996) defined

$$\lambda_{\rm eff} = \exp \langle \ln \lambda \rangle = \exp \frac{\int (\ln \lambda) S(\nu) d(\ln \nu)}{\int S(\nu) d(\ln \nu)}, \quad \text{(A26)}$$

which is not flux-averaged as is the $\lambda_{\rm eff}$ of Schneider et al. (1983). To further complicate definitions, Doi et al. (2010) defined

$$\lambda_{\rm eff} = \frac{c}{\nu_{\rm eff}}, \quad \text{(A27)}$$

where

$$\nu_{\rm eff} = \frac{\int \nu S(\nu) d\nu/h\nu}{\int S(\nu) d\nu/h\nu} = \frac{\int \nu S'(\nu) d\nu}{\int S'(\nu) d\nu}. \quad \text{(A28)}$$

Equation (A28) is the definition of the mean energy-weighted frequency, not the mean (effective [sic]) photon-weighted frequency as stated by Doi et al. (2010). Footnote 13 in that article is also in error.

The "effective" frequency defined by Doi et al. (2010) is the "mean" frequency defined by Koornneef et al. (1986) and not the usual definition of the flux-weighted "effective" frequency similar to the Schneider et al. (1983) "effective" frequency.

For comparison we evaluate the labeled wavelengths for the V band and Vega. Some, such as $\lambda_{\rm eff}$, involve the product of the stellar flux and the system response function, while others such as λ_p and λ_0 concern the system response passband only. Some of the different labeled photon-counting wavelength values are $(\lambda_{\rm eff}, \lambda_{\rm iso}, \lambda_p) = (5455\ \text{Å}, 5486\ \text{Å}, 5488\ \text{Å})$. The mean photon wavelength $\lambda_0 = 5499$ Å, compared with the mean energy

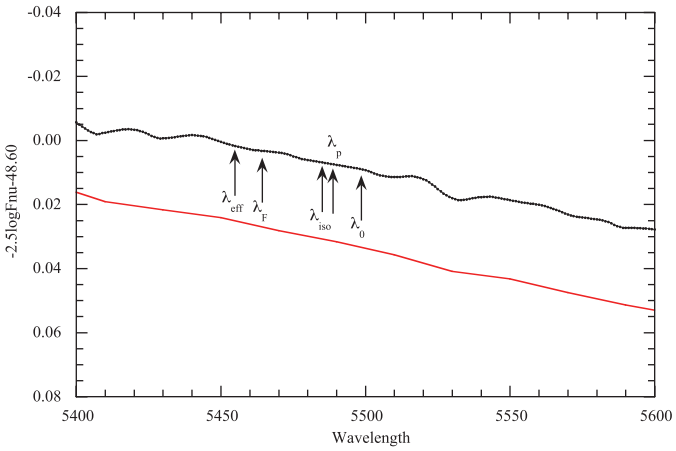

FIG. 17.—STIS005 f_ν spectrum of Vega (*black*) with some specific wavelengths marked (*see text*). The λ_F is the Fukugita et al. (1996) $\lambda_{\rm eff}$. The STIS005 spectrum yields $V = 0.007$ mag. The line is the Castelli 1994 Vega model flux scaled by 1.2876×10^{15} to produce $V = 0.03$ mag. See the electronic edition of the *PASP* for a color version of this figure.

TABLE 6
CROSS-REFERENCE OF PHOTOMETRIC TERMS

Name	Description	synphot	pysynphot	Equation
R	Predetector response function	...	...	...
S	Photon response function	P_λ	P_λ = spectral element = bp	(A6)
S'	Energy response function	λP_λ[a]	λP_λ	(A9)
λ_0	Mean wavelength	avgwv	bp.avgwave	(A14)
λ_p	Pivot wavelength	pivwv	bp.pivot	(A16)
$\lambda_{\rm eff}$	Effective wavelength	efflam	Observation.efflam	(A21)
$\lambda^*_{\rm eff}$	Schneider et al. (1983) $\lambda_{\rm eff}$	barlam	...	(A25)
f_λ	flambda	flam	Observation.effstim(flam)	...
f_ν	fnu	fnu	Observation.effstim(fnu)	...
AB_ν	$-2.5\log\langle f_\nu\rangle - 48.60$[b]	abmag	Observation.effstim(abmag)	(A3)
AB_λ	$-2.5\log\langle f_\lambda\rangle - 21.10$[c]	stmag	Observation.effstim(stmag)	(A4)

[a] λP_λ used here is a normalized quantity (made by dividing by the peak wavelength).
[b] -48.60 (Oke & Gunn 1983) used in synphot and pysynphot.
[c] -21.10 (Oke & Gunn 1983) used in synphot and pysynphot.

wavelength $\lambda'_0 = 5524$ Å. The Schneider et al. (1983) $\lambda^*_{\rm eff} = 5444$ Å, the Fukugita et al. (1996) $\lambda_{\rm eff} = 5464$ Å, and the Doi et al. (2010) $\lambda_{\rm eff} = 5453$ Å. We have marked some of these wavelengths in Figure 17, showing the f_ν flux (in magnitudes) of Vega between 5400 Å and 5600 Å.

This illustrates the unnecessary confusion of these weighted wavelengths. We recommend the retention of only two: the pivot wavelength, λ_p, which is a property of the passband only, and the isophotal wavelength, $\lambda_{\rm iso}$, which takes into account the spectrum measured. To better quantify the derivation of the isophotal wavelength, we recommend that the flux be smoothed to a resolution of one-third of the FWHM of the passband. The pivot wavelength should be used as part of a description of the filter system, while the isophotal wavelength should be used to plot the fluxes as broadband magnitudes against wavelength.

A2.2. Equations Involving Observed Fluxes

Following Oke & Gunn (1983), Fukugita et al. (1996), and Doi et al. (2010), we defined the broadband AB magnitude as

$$\begin{aligned}\text{AB magnitude} &= -2.5\log\langle f_\nu\rangle - 48.60\\ &= -2.5\log\left(\frac{\int f_\nu(\nu)S(\nu)d\nu/\nu}{\int S(\nu)d\nu/\nu}\right) - 48.60.\end{aligned} \tag{A29}$$

Fukugita et al. (1996) imply that this is a photon-counting magnitude; however, the preceding equation is the energy-integration equation (see eq. [A12]; as discussed previously, based on the Vega STIS005 spectrum, the constant should be -48.577 to be on the same magnitude scale as the V system for $V_{\rm vega} = 0.03$).

Equation (A13) shows that photon-counting and energy-integration magnitudes were equivalent, but with different offset constants that are subsumed in the standardization process. That is, the apparent observed magnitude is usually defined as

$$\begin{aligned}m_j &= C_j - 2.5\log\int n_p(\lambda)S(\lambda)d\lambda\\ &= C'_j - 2.5\log\int f_\lambda(\lambda)S(\lambda)\lambda d\lambda,\end{aligned} \tag{A30}$$

with the constants C_j or C'_j found from photometric standards. Note that the first integral describes photon-counting, while the second integral describes energy integration. The regular appearance of the (normalized) product $S(\lambda)\lambda$ in integrals pertaining to photometric magnitudes is often explained simply as wavelength weighting the response function to account for photon-counting; however, it is primarily a consequence of the modern practice of using the photon response functions, rather than the energy response functions used in the past.

The most important reason for maintaining the contemporary practice of using photonic response functions is the fact that they are the default response functions in commonly used data reductions packages, such as synphot and pysynphot. All the passbands published in this article are photonic passbands $S(\lambda)$.

A2.3. Synphot and Pysynphot

The *HST* photometry packages synphot[15] and pysynphot[16] are commonly used for planning *HST* observations and synthetic photometry. It is useful to relate the definitions, variable names, and labels in these packages to those used in this article. Table 6 is a cross-reference list of terms.

[15] See http://stsdas.stsci.edu/stsci_python_epydoc/SynphotManual.pdf.
[16] See http://stsdas.stsci.edu/pysynphot/.

REFERENCES

Azusienis, A., & Straizys, V. 1969, Soviet Astron., 13, 316
Bessell, M. S. 1983, PASP, 95, 480
———. 1986, PASP, 98, 1303
———. 1990a, PASP, 102, 1181
———. 1990b, A&AS, 83, 357
———. 2000, PASP, 112, 961
———. 2011, PASP, 123, 1442
Bessell, M. S., & Brett, J. M. 1988, PASP, 100, 1134
Bessell, M. S., Castelli, F., & Plez, B. 1998, A&A, 323, 231
Bohlin, R. C., & Gilliland, R. L. 2004, AJ, 127, 3508
Bohlin, R. C. 2007, in ASP Conf. Ser. 364, The Future of Photometric, Spectrophotometric, and Polarimetric Standardization, ed. C. Sterken (San Francisco: ASP), 315
Buser, R. 1986, Highlights Astron., 7, 799
Buser, R., & Kurucz, R. L. 1978, A&A, 70, 555
Cohen, M., Walker, R. G., Barlow, M. J., & Deacon, J. R. 1992, AJ, 104, 1650
Cousins, A. W. J. 1974, MNRAS, 166, 711
———. 1976, MmRAS, 81, 25
———. 1984, SAAO Circ, 8, 69
Cousins, A. W. J., & Menzies, J. W. 1993, in Precision Photometry, ed. D. Kilkenny, E. Lastovica, & J. W. Menzies. (Cape Town: SAAO), 240
Doi, M., Tanaka, M., Fukugita, M., Gunn, J. E., Yasuda, N., Ivezic, Z., Brinkmann, J., de Haars, E., et al. 2010, AJ, 139, 1628
Fukugita, M., Ichikawa, T., Gunn, J. E., Doi, M., Shimasaku, K., & Schneider, D. P. 1996, AJ, 111, 1748
Gray, R. O. 2007, in ASP Conf. Ser. 364, The Future of Photometric, Spectrophotometric, and Polarimetric Standardization, ed. C. Sterken (San Francisco: ASP), 305
Gronbech, B., & Olsen, E. H. 1976, A&AS, 34, 1
Gustafsson, B., Edvardsson, B., Eriksson, K., Jorgensen, U. G., Nordlund, A., & Plez, B. 2008, A&A, 486, 951
Hayes, D. S. 1985, in IAU Symp. 111, Calibration of Fundamental Stellar Quantities, ed. D. S. Hayes, L. E. Pasinetti, & A. G. Davis Philip (Dordrecht: Reidel), 225
Heap, S. R., & Lindler, D. 2007, in IAU Symp. 241, Stellar Populations as Building Blocks of Galaxies (Cambridge: Cambridge Univ. Press),95
Hog, E., Fabricius, C., Makarov, V. V., Urban, S., Corbin, T., Wycoff, G., Bastian, U., Schwekendiek, P., et al. 2000, A&A, 355, L27
Johnson, H. L., Iriarte, B., Mitchell, R. I., & Wisniewski, W. Z. 1966, Commun. Lunar Planet. Lab., 4, 99
Kaiser, N. , Burgett, W., Chambers, K., Denneau, L., Heasley, J., Jedicke, R., Magnier, E., Morgan, J., et al. 2010, Proc. SPIE, 7733, 77330E1
Keller, S., et al. 2007, PASA, 24, 1
King, I. 1952, ApJ, 115, 580
Kilkenny, D., van Wyk, F., Roberts, G., Marang, F., & Cooper, D. 1998, MNRAS, 294, 93
Koen, C., Kilkenny, D., van Wyk, F., Cooper, D., & Marang, F. 2002, MNRAS, 334, 20
Koen, C., Kilkenny, D., van Wyk, F., & Marang, F. 2010, MNRAS, 403, 1949
Koornneef, J., Bohlin, R., Buser, R., Horne, K., & Turnshek, D. 1986, Highlights Astron., 7, 833
Landolt, A.U. 1983, AJ, 88, 439
———. 2009, AJ, 137, 4186
Landolt, A. U., & Uomoto, A. K. 2007, AJ, 133, 768
MaizApellaniz, J. 2006, AJ, 131, 1184
Megessier, C. 1995, A&A, 296, 771
Menzies, J. W., Cousins, A. W. J., Banfeld, R. M., & Laing, J. D. 1989, SAAO Circ, 13, 1
———. 1993, in Precision Photometry, ed. D. Kilkenny, E. Lastovica, & J. W. Menzies (Cape Town: SAAO), 35
Munari, U., Sordo, R., Castelli, F., & Zwitter, T. 2005, A&A, 442, 1127
Nicolet, B. 1978, A&AS, 34, 1
———. 1996, Baltic Astron., 5, 417
Olsen, E. H. 1983, A&AS, 54, 55
Oke, J. B. 1965, ARA&A, 3, 23
Oke, J. B., & Gunn, J. E. 1983, ApJ, 266, 713
Oke, J. B., & Schild, R. E. 1970, ApJ, 161, 1015
Pel, J.-W., & Lub, J. 2007, in ASP Conf. Ser. 364, The Future of Photometric, Spectrophotometric and Polarimetric Standardization (San Francisco: ASP), 63
Perryman, M. A. C., Lindegren, L., Kovalevsky, J., Hog, E., Bastian, U., Bernacca, P. L., Creze, M., Donati, F., et al. 1997, A&A, 323, L49
Rufener, F., & Nicolet, B. 1988, A&A, 206, 357
Sanchez-Blazquez, P., Peletier, R. F., Jimenez-Vicente, J., Cardiel, N., Cenarro, A. J., Falcon-Barroso, J., Gorgas, J., Selam, S., et al. 2006, MNRAS, 371, 703
Schneider, D. P., Gunn, J. E., & Hoessel, J. G. 1983, ApJ, 264, 337
Soffer, B. H., & Lynch, D. K. 1999, Am. J. Phys., 67, 946
Straižys, V. 1996. Baltic Astron., 5, 459
Straizys, V., & Sviderskiene, Z. 1972, Vilnius Astron. Obs. Biuletenis, 35, 3
Tokunaga, A. T., & Vacca, W. D. 2005, PASP, 117, 421
van Leeuwen, F., Evans, D. W., Grenon, M., Grossmann, V., Mignard, F., & Perryman, M. A. C. 1997, A&A, 323, L61
van Leeuwen, F., Lindegren, L., & Mignard, F. 1997, The *Hipparcos* and Tycho Catalogues, (ESA SP-1200; Noordwijk: ESA), 3, 461